Secure SWIPT for Directional Modulation-Aided AF Relaying Networks

Xiaobo Zhou, Jun Li, *Senior Member, IEEE*, Feng Shu, *Member, IEEE*, Qingqing Wu, *Member, IEEE*, Yongpeng Wu, *Senior Member, IEEE*, Wen Chen, *Senior Member, IEEE*, and Lajos Hanzo, *Fellow, IEEE*

***Abstract*— Secure wireless information and power transfer based on directional modulation is conceived for amplify-and-forward relaying networks. Explicitly, we first formulate a secrecy rate maximization (SRM) problem, which can be decomposed into a twin-level optimization problem and solved by a one-dimensional (1D) search and semidefinite relaxation (SDR) technique. Subsequently, in order to reduce the search complexity, we formulate an optimization problem based on maximizing the signal-to-leakage-AN-noise-ratio (Max-SLANR) criterion, and transform it into a SDR problem. In addition, the relaxation is proved to be tight according to the classic Karush-Kuhn-Tucker (KKT) conditions. Finally, to reduce the computational complexity, a successive convex approximation (SCA) scheme is proposed to find a near-optimal solution. The complexity of the SCA scheme is much lower than that of the SRM and the Max-SLANR schemes. Simulation results demonstrate that the performance of the SCA scheme is very close to that of the SRM scheme in terms of its secrecy rate and bit error rate, but much better than that of the zero forcing scheme.**

***Index Terms*— Directional modulation, simultaneous wireless information and power transfer, AF, artificial noise, secrecy rate.**

Manuscript received March 15, 2018; revised July 05, 2018; accepted September 06, 2018. Date of publication October 2, 2018; date of current version January 15, 2019. This work was supported in part by the National Key R&D Program under Grant 2018YFB1004802, in part by the National Natural Science Foundation of China under Grant 61872184, Grant 61801453, Grant 61771244, Grant 61727802, Grant 61702258, Grant 61501238, Grant 61472190, and Grant 61271230, in part by the Jiangsu Provincial Science Foundation under Project BK20150786, in part by the Specially Appointed Professor Program in Jiangsu Province, in 2015, in part by the Fundamental Research Funds for the Central Universities under Grant 30916011205, and in part by the Open Research Fund of National Mobile Communications Research Laboratory, Southeast University, under Grant 2017D04. The work of L. Hanzo was supported in part by EPSRC under Project EP/Noo4558/1 and Project EP/PO34284/1 and in part by the European Research Council's Advanced Fellow Grant QuantCom. *(Corresponding authors: Jun Li; Feng Shu.)*

X. Zhou is with the School of Electronic and Optical Engineering, Nanjing University of Science and Technology, Nanjing 210094, China, and also with the School of Fuyang Normal University, Fuyang 236037, China (e-mail: zxb@njust.edu.cn).

J. Li is with the School of Electronic and Optical Engineering, Nanjing University of Science and Technology, Nanjing 210094, China, also with the National Mobile Communications Research Laboratory, Southeast University, Nanjing 210018, China, and also with the School of Computer Science and Robotics, National Research Tomsk Polytechnic University, 634050 Tomsk, Russia (e-mail: jun.li@njust.edu.cn).

F. Shu is with the School of Electronic and Optical Engineering, Nanjing University of Science and Technology, Nanjing 210094, China (e-mail: shufeng0101@163.com).

Q. Wu is with the Department of Electrical and Computer Engineering, National University of Singapore, Singapore 117583 (e-mail: elewuqq@nus.edu.sg).

Y. Wu and W. Chen are with the Department of Electronic Engineering, Shanghai Institute of Advanced Communications and Data Sciences, Shanghai Jiao Tong University, Minhang 200240, China (e-mail: yongpeng.wu@sjtu.edu.cn; wenchen@sjtu.edu.cn).

L. Hanzo is with the Department of Electronics and Computer Science, University of Southampton, Southampton SO17 1BJ, U.K. (e-mail: lh@ecs.soton.ac.uk).

Color versions of one or more of the figures in this paper are available online at http://ieeexplore.ieee.org.

Digital Object Identifier 10.1109/JSAC.2018.2872372

I. Introduction

THE past decade has witnessed the rapid development of the Internet of Things (IoT). It is forecast that by 2025 about 30 billion IoT devices will be used worldwide [1]. Since using conventional batteries is inconvenient for such a huge number of devices, simultaneous wireless information and power transfer (SWIPT) is recognized as a promising technology to prolong the operation time of wireless devices [2]–[12]. The separated information receiver (IR) and energy receiver (ER) are considered in [2]–[4]. Son and Clerckx [2] considered a multi-user wireless information and power transfer system, where the beamforming vector was designed by the zero-forcing (ZF) algorithm and updated by maximizing the energy harvested. In [3], the optimal beamforming scheme was proposed for achieving the maximum secrecy rate, while meeting the minimum energy requirement at the ER. Zhang *et al.* [4] designed robust information and energy beamforming vectors for maximizing the energy harvested by the ER under specific constraints on the signal-to-interference plus noise ratio (SINR) at the IR. A power splitting (PS) scheme was utilized to divide the received signal into two parts in order to simultaneously harvest energy and to decode information [5]–[8]. Zhou *et al.* [9] and Zhang and Ho [10] investigated both PS and time switching (TS) schemes and compared the performance of these two schemes.

As an important technique of expanding the coverage of networks, relaying can also beneficially enhance the communication security, whilst simultaneously enhancing energy harvesting [13]–[19]. An innovative SWIPT scheme was conceived for a non-regenerative multiple-input multiple-output orthogonal frequency-division multiplexing (MIMO-OFDM) relaying system in [13], while a two-hop self-sustained amplify-and-forward (AF) relay arrangement was considered in [14]. For the case of perfect channel state information (CSI) situations, secure SWIPT invoked in relaying networks has been investigated [20]–[22]. Authors of [20] proposed a constrained concave convex procedure (CCCP)-based iterative algorithm for designing the beamforming vector of multi-antenna aided non-regenerative relay networks, while in [21], the analytical expressions of the ergodic secrecy capacity were

derived separately based on TS, PS and on ideal relaying protocols. As a further development, the beamforming vectors of SWIPT were designed for AF two-way relay networks through a sequential parametric convex approximation (SPCA)-based iterative algorithm to find its locally optimal solution in [22].

By contrast, a suitable channel estimation uncertainty model was considered in [23]–[29] for realistic imperfect CSI scenarios. In [23] and [24], a more general robust beamformer was designed for coping with the mismatch between the true and the estimated steering vectors. In [25]–[27], a robust information beamformer and artificial noise (AN) covariance matrix were designed with the objective of maximizing the secrecy rate under the constraint of a certain maximum transmit power. The secrecy rate maximization (SRM) problem was a nonconvex problem in [25]–[27], where the cardinal question is, how to transform it into a tractable convex optimization problem by using the S-Procedure. In [28] and [29], the authors formulate the power minimization problem under a specific secrecy rate constraint and minimum energy requirement at the energy harvester (EH), which was solved in a similar manner. In general, for the imperfect CSI situations, the channel estimation error is usually modeled the so-called ellipsoid bound constraint, and then it is transformed into a convex constraint by using the S-procedure.

Recently, a promising physical layer security technique, known as directional modulation (DM), has attracted a lot of attention. In contrast to conventional information beamforming techniques, DM has the ability to directly transmit the confidential messages in desired directions to guarantee the security of information transmission, while distorting the signals leaking out in other directions [30]–[34]. Daly and Bernhard [30] proposed a DM technique that employed a phased array to generate the modulation. By controlling the phase shift for each array element, the magnitude and phase of each symbol can be adjusted for radiating in the desired direction. Ding and Fusco [31] proposed a method relying on orthogonal vectors and introduced the concept of AN into DM systems and synthesis. Since the AN contaminates the undesired receiver, the security of the DM systems is greatly improved. Subsequently, the orthogonal vector based method was invoked by multi-beam DM systems [32]. The methods proposed in [31] and [32] achieve better performance at the perfect direction angle, but they are very sensitive to the estimation error of the direction angle. Hu *et al.* [33] modeled the error of angle estimation by a uniform distribution and proposed a robust synthesis method for the DM system to reduce the effect of estimation error. Shu *et al.* [34] also considered the estimation error of the direction angle and proposed a robust beamforming scheme for a DM broadcast scenario.

However, none of these contributions consider DM-based relaying techniques. For example, if the desired user is beyond the coverage of the transmitter or there is no direct link between the transmitter and the desired user, the above methods are not applicable. Moreover, the robust methods proposed in [33] and [34] only designed the normalized beamforming and AN projection matrix without considering the power allocation problem. In fact, the power allocation of confidential messages and AN has a grave impact on the security of DM systems. However, to the best of our knowledge, there exists no DM-based scheme considering secure SWIPT, which thus motivates this work.

To tackle this open problem, we propose a secure SWIPT scheme based on AF relay aided DM. Compared to [25]–[29], instead of using the channel estimation error model obeying the ellipsoid bound constraint, we model the estimation error of the direction angle as the truncated Gaussian distribution, which is more practical in our DM scenario [34]. **The main contributions of this paper are summarized as follows**.

1) We formulate the SRM problem subject to the total power constraint at an AF relay and to the minimum energy requirement at the ER. Since the secrecy rate expression is the difference of two logarithmic functions, it is noncovex and hence it is difficult to tackle directly. Additionally, the estimates of the eavesdropper directions are usually biased. To solve this problem and to find the robust information beamforming matrix as well as the AN covariance matrix, we convert the original problem into a twin-level optimization problem, which can be solved by a one-dimensional (1D) search and the classic semidefinite relaxation (SDR) technique. The 1D search range is bounded into a feasible interval. Furthermore, the SDR is proved to be tight by invoking the Karush-Kuhn-Tucker (KKT) conditions.

2) To reduce the search complexity, we propose a suboptimal solution for maximizing the signal-to-leakage-AN-noise-ratio (Max-SLANR) subject to the total power constraint of the relay and to the minimum energy required at the ER. Due to the existence of multiple eavesdroppers, we consider the sum-power of the confidential messages leaked out to all the eavesdroppers. This optimization problem is also shown to be nonconvex, but it can be transformed into a semidefinite programming (SDP) problem and then solved by the SDR technique. Its tightness is also quantified. To further reduce the computational complexity, we propose an algorithm based on successive convex approximation (SCA). Specifically, we first formulate the SRM optimization problem and then transform it into a second-order cone programming (SOCP), which is finally solved by the SCA method. Furthermore, we analyse and compare the complexity of the aforementioned three schemes.

3) The formulated optimization problems include random variables corresponding to the estimation error of the direction angles, which makes the optimization problems very difficult to tackle directly. To facilitate solving this problem, we derive the analytical expression of the covariance matrix of each eavesdroppers' steering vector and substitute it into the optimization problems to replace the random variable. Moreover, we add relays and energy harvesting nodes to the DM-based secure systems, which further expand the application of DM technology. Simulation results demonstrate that the bit error rate (BER) performance of all our schemes in the desired direction is significantly better than that in other directions, while the BER is poor in the vicinity of the eavesdroppers' directions, showing the advantages of our DM technology in the field of physical layer security.

It is worth noting that a robust and secure beamforming design of multiple cooperating AF relays was studied in [35],

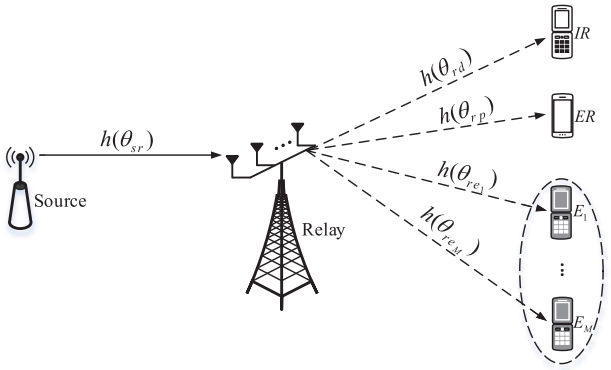

Fig. 1. System model of secure beamforming with SWIPT based on directional modulation in AF relaying networks

where the channel estimation error was assumed to be within a ellipsoid. The main differences between our manuscript and [35] are as follows: 1) We introduce an AF relay into the DM system to extend the DM application scenarios as well as to enhance the security of the system. 2) Our DM system considers the scenario where there is an estimation error of the direction angles at the relay. Furthermore, we design robust as well as secure beamforming by deriving the covariance matrix of the eavesdroppers¡¯ channels. By contrast, our Colleagues in [35] considered the deleterious effects of channel estimation errors and assumed that the estimation errors were confined within an ellipsoid. 3) We focus our attention on the robust as well as secure beamforming design with the consideration of power transfer, while it is not considered in [35].

The rest of this paper is organized as follows. Section II introduces the system model. In Section III, three algorithms are proposed for designing our robust secure beamforming. Section IV provides our simulation results, while, Section V concludes the paper.

Notation: Boldface lowercase and uppercase letters represent vectors and matrices, respectively, $\mathbf{A}^*$, $\mathbf{A}^T$, $\mathbf{A}^H$, $\mathrm{Tr}(\mathbf{A})$, $\mathrm{rank}(\mathbf{A})$, $\mathbf{A} \succ \mathbf{0}$ and $\mathbf{A} \succeq \mathbf{0}$ denote conjugate, transpose, conjugate transpose, trace, rank, positiveness and semidefiniteness of matrix $\mathbf{A}$, respectively, $\mathbb{E}[\cdot]$, j, and $\|\cdot\|$ denote the statistical expectation, pure imaginary number, and Euclidean norm, respectively, and $\otimes$ denotes the Kronecker product.

II. System Model

As shown in Fig. 1, we consider AF-aided secure SWIPT, where the source transmitter sends confidential messages to an IR with the aid of an AF relay in the presence of an ER and M eavesdroppers $(\mathrm{E}_1, \cdots, \mathrm{E}_M)$. It is assumed that the AF relay is equipped with an N-element antenna array, while all other nodes have a single antenna. This assumption is satisfied in numerous application scenarios. For example, when the transmitter and the receiver, each equipped with a single antenna, are located on the ground, the direct links between them may be considered to be blocked due to the substantial path loss in a worst-case scenario due to large-bodied obstacles. An unmanned aerial vehicle (UAV) equipped with multiple antennas is assigned as a relay to support the communications of the designated nodes and transfer power to other nodes in the meantime.

Similar to the literature on DM [33], [34], this paper adopts the free-space path loss model which is practical for some scenarios such as communication in the air and rural areas.

The steering vector between node a and node b can be expressed as [31]

$$\mathbf{h}(\theta_{ab}) = \sqrt{g_{ab}} \underbrace{\frac{1}{\sqrt{N}} \left[e^{j2\pi\Psi_{\theta_{ab}}(1)}, \cdots, e^{j2\pi\Psi_{\theta_{ab}}(N)}\right]^T}_{\text{The normalized steering vector}}, \quad (1)$$

where g_{ab} is the path loss between node a and node b. The function $\Psi_{\theta_{ab}}(n)$ can be expressed as

$$\Psi_{\theta_{ab}}(n) \triangleq -\frac{(n-(N+1)/2)l\cos\theta_{ab}}{\lambda}, \quad n = 1, \ldots, N, \quad (2)$$

where θ_{ab} denotes the angle of direction between node a and node b, l denotes the distance between two adjacent antenna elements, and λ is the wavelength.

We note that leakage may be encountered both along the line-of-sight (LOS) and non-line-of-sight (NLOS) paths. However, compared to the information leakage from the LOS paths, the NLOS paths leakage may be deemed negligible due to the severe path loss. Additionally, the eavesdroppers are motivated to exploit the LOS channels so as to glean as much information as they can from the transmitter. In this sense, it is reasonable to assume having LOS channels between the relay and the eavesdroppers.

We assume that there is no direct link from the source to the IR, ER or to any of the eavesdroppers. This occurs in the worst-case scenario, when the direct links are blocked due to the high path loss imposed by obstacles. Thus the relay helps the source to transmit the confidential message x to IR. The relay node is assumed to operate in an AF half-duplex mode. Simultaneously, ER intends to harvest energy, while the eavesdroppers try to intercept the confidential messages. The power of the signal x is normalized to, $\mathbb{E}[xx^H] = 1$. In the first time slot, the source transmits the signal x to the relay, and the signal received at the relay is given by

$$\mathbf{y}_r = \sqrt{P_s}\mathbf{h}(\theta_{sr})x + \mathbf{n}_r, \quad (3)$$

where P_s is the transmission power of the source, $\mathbf{h}(\theta_{sr})$ denotes the steering vector between the source and the relay, $\mathbf{n}_r \sim \mathcal{CN}(0, \sigma_r^2\mathbf{I}_N)$ is a circularly symmetric complex Gaussian (CSCG) noise vector, and θ_{sr} is the angle of direction between the source and the relay. In the second time slot, the relay amplifies and forwards the received signal to IR. The signal transmitted from the relay is given by

$$\mathbf{x}_r = \mathbf{W}\mathbf{y}_r + \mathbf{z} = \sqrt{P_s}\mathbf{W}\mathbf{h}(\theta_{sr})x + \mathbf{W}\mathbf{n}_r + \mathbf{z}, \quad (4)$$

where $\mathbf{W} \in \mathbb{C}^{N\times N}$ is the beamforming matrix, and $\mathbf{z} \in \mathbb{C}^{N\times 1}$ is the AN vector assumed to obey a (CSCG) distribution $\mathcal{CN}(0, \mathbf{\Omega})$ with $\mathbf{\Omega} \succeq 0$. In general, the relay has a total transmit power constraint P_t, therefore we have

$$P_s\|\mathbf{W}\mathbf{h}(\theta_{sr})\|^2 + \sigma_r^2\mathrm{Tr}(\mathbf{W}^H\mathbf{W}) + \mathrm{Tr}(\mathbf{\Omega}) \le P_t. \quad (5)$$

The signal received at the IR, ER, and the m-th eavesdropper can be expressed as

$$\begin{aligned} y_d &= \mathbf{h}^H(\theta_{rd})\mathbf{x}_r + n_0 \\ &= \sqrt{P_s}\mathbf{h}^H(\theta_{rd})\mathbf{W}\mathbf{h}(\theta_{sr})x + \mathbf{h}^H(\theta_{rd})\mathbf{W}\mathbf{n}_r \\ &\quad + \mathbf{h}^H(\theta_{rd})\mathbf{z} + n_0, \end{aligned} \tag{6}$$

$$\begin{aligned} y_p &= \sqrt{P_s}\mathbf{h}^H(\theta_{rp})\mathbf{W}\mathbf{h}(\theta_{sr})x + \mathbf{h}^H(\theta_{rp})\mathbf{W}\mathbf{n}_r \\ &\quad + \mathbf{h}^H(\theta_{rp})\mathbf{z} + n_p, \end{aligned} \tag{7}$$

and

$$\begin{aligned} y_{e_m} = \sqrt{P_s}\mathbf{h}^H(\theta_{re_m})\mathbf{W}\mathbf{h}(\theta_{sr})x + \mathbf{h}^H(\theta_{re_m})\mathbf{W}\mathbf{n}_r \\ + \mathbf{h}^H(\theta_{re_m})\mathbf{z} + n_e, \quad m \in \mathcal{M} = [1, 2, ..., M], \end{aligned} \tag{8}$$

respectively, where $\mathbf{h}(\theta_{rd})$, $\mathbf{h}(\theta_{rp})$, and $\mathbf{h}(\theta_{re_m})$ denote the steering vectors from the relay to IR, ER, and the m-th eavesdropper respectively. Furthermore, n_0, n_p, and n_e represent the CSCG noise at IR, ER, and the m-th eavesdropper, respectively, while $n_0 \sim \mathcal{CN}(0, \sigma_0^2)$, $n_p \sim \mathcal{CN}(0, \sigma_k^2)$, and $n_e \sim \mathcal{CN}(0, \sigma_e^2)$. Without loss of generality, we assume that σ_r^2, σ_0^2, σ_k^2, and σ_e^2 are all equal to σ^2.

Similar to the considerations in [26] and [28], namely that the perfect CSI of the destination is available at the relay, here we assume that the relay has the perfect knowledge of direction angles to the IR. However, there is an estimation error of the direction angles of eavesdroppers at the relay, and we assume that the relay has the statistical information about these estimation errors. Therefore, the m-th eavesdropper's direction angle to the relay can be modeled as

$$\theta_{re_m} = \hat{\theta}_{re_m} + \Delta\theta_{re_m}, m \in \mathcal{M}, \tag{9}$$

where $\hat{\theta}_{re_m}$ is the estimate of the m-th eavesdropper's direction angle at the relay, and $\Delta\theta_{re_m}$ denotes the estimation error, which is assumed to follow a truncated Gaussian distribution spread over the interval $[-\Delta\theta_{max}, \Delta\theta_{max}]$ with zero mean and variance σ_θ^2. The probability density function of $\Delta\theta_{re_m}$ can be expressed as

$$f(\Delta\theta_{re_m}) = \begin{cases} \dfrac{1}{K_e\sqrt{2\pi}\sigma_\theta} e^{\dfrac{-\Delta\theta_{re_m}^2}{2\sigma_\theta^2}}, & -\Delta\theta_{max} \le \Delta\theta_{re_m} \le \Delta\theta_{max}, \\ 0, & \text{otherwise}, \end{cases} \tag{10}$$

where K_e is the normalization factor defined as

$$K_e = \int_{-\Delta\theta_{max}}^{\Delta\theta_{max}} \frac{1}{\sqrt{2\pi}\sigma_\theta} e^{\frac{-\Delta\theta_{re_m}^2}{2\sigma_\theta^2}} d(\Delta\theta_{re_m}). \tag{11}$$

III. Robust Secure SWIPT Design

In this section, three algorithms are proposed to design the robust secure beamforming under the assumption that an estimation error of the direction angles of eavesdroppers exists at the relay. To design the robust beamforming matrix and AN covariance matrix, we first define

$$\mathbf{H}_{re_m} \triangleq \mathbb{E}_{\Delta\theta_{re_m}}\left[\mathbf{h}(\hat{\theta}_{re_m} + \Delta\theta_{re_m})\mathbf{h}^H(\hat{\theta}_{re_m} + \Delta\theta_{re_m})\right], \tag{12}$$

where $m \in \mathcal{M}$, and $\mathbf{H}_{re_m} \in \mathbb{C}^{N\times N}$. Let $H_{re_m}(p,q)$ denote the p-th row and q-th column entry of $\mathbf{H}_{re_m}$, and $H_{re_m}(p,q)$ can be written as

$$H_{re_m}(p,q) = \Gamma_{1_m}(p,q) - j\Gamma_{2_m}(p,q), \tag{13}$$

where Γ_{1_m} and Γ_{2_m} can be found in (64) and (67), respectively. The specific derivation procedure is detailed in Appendix A.

According to (7), the energy harvested at the ER is given by [36]

$$\begin{aligned} E = \rho\big[P_s|\mathbf{h}^H(\theta_{rp})\mathbf{W}\mathbf{h}(\theta_{sr})|^2 + \sigma^2\|\mathbf{W}^H\mathbf{h}(\theta_{rp})\|^2 \\ + \mathbf{h}^H(\theta_{rp})\mathbf{\Omega}\mathbf{h}(\theta_{rp})\big], \end{aligned} \tag{14}$$

where $0 < \rho \le 1$ denotes the energy transfer efficiency of the ER.

From (6), the SINR at the IR can be expressed as

$$\mathrm{SINR}_d = \frac{P_s|\mathbf{h}^H(\theta_{rd})\mathbf{W}\mathbf{h}(\theta_{sr})|^2}{\sigma^2\|\mathbf{W}^H\mathbf{h}(\theta_{rd})\|^2 + \mathbf{h}^H(\theta_{rd})\mathbf{\Omega}\mathbf{h}(\theta_{rd}) + \sigma^2}. \tag{15}$$

According to (8), the m-th eavesdropper's SINR is given by

$$\mathrm{SINR}_{e_m} = \frac{P_s|\mathbf{h}^H(\theta_{re_m})\mathbf{W}\mathbf{h}(\theta_{sr})|^2}{\sigma^2\|\mathbf{W}^H\mathbf{h}(\theta_{re_m})\|^2 + \mathbf{h}^H(\theta_{re_m})\mathbf{\Omega}\mathbf{h}(\theta_{re_m}) + \sigma^2}. \tag{16}$$

Since we assume that there is an estimation error of the direction angles of the eavesdroppers at the relay and the relay only has the statistical information about these estimation errors. Thus, the average secrecy rate can be defined as [37], [38]

$$\begin{aligned} R_s &= \min_{m\in\mathcal{M}}\Big\{\mathbb{E}_{\Delta\theta_{re_m}}\big[\frac{1}{2}\log_2(1+\mathrm{SINR}_d) \\ &\qquad - \frac{1}{2}\log_2(1+\mathrm{SINR}_{e_m})\big]\Big\}, \end{aligned} \tag{17a}$$

$$\begin{aligned} &= \min_{m\in\mathcal{M}}\Big\{\frac{1}{2}\log_2(1+\mathrm{SINR}_d) \\ &\qquad - \mathbb{E}_{\Delta\theta_{re_m}}\big[\frac{1}{2}\log_2(1+\mathrm{SINR}_{e_m})\big]\Big\}, \end{aligned} \tag{17b}$$

where (17b) is valid, because the first term of (17a) is independent of the random variable $\Delta\theta_{re_m}$, and the scaling factor $\frac{1}{2}$ is due to the fact that two time slots are required to transmit one message. By invoking Jensen's inequality, the worst-case secrecy rate is given by

$$\begin{aligned} R_s \ge \bar{R}_s = \min_{m\in\mathcal{M}}\frac{1}{2}\Big\{\log_2(1+\mathrm{SINR}_d) \\ - \log_2\big(1+\mathbb{E}_{\Delta\theta_{re_m}}\big[\mathrm{SINR}_{e_m}\big]\big)\Big\}, \end{aligned} \tag{18}$$

where the expectation of the $\mathrm{SINR}_{\mathrm{em}}$ can be approximated as [39], [40]

$$\begin{aligned} &\mathbb{E}_{\Delta\theta_{re_m}}[\mathrm{SINR}_{e_m}] \\ &\approx \frac{\mathbb{E}_{\Delta\theta_{re_m}}[P_s|\mathbf{h}^H(\theta_{re_m})\mathbf{W}\mathbf{h}(\theta_{sr})|^2]}{\mathbb{E}_{\Delta\theta_{re_m}}[\sigma^2\|\mathbf{W}^H\mathbf{h}(\theta_{re_m})\|^2] + \mathbb{E}[\mathbf{h}^H(\theta_{re_m})\mathbf{\Omega}\mathbf{h}(\theta_{re_m})] + \sigma^2}. \end{aligned} \tag{19}$$

A. Secrecy Rate Maximization Based on One-Dimensional Search Scheme (SRM-1D)

In this subsection, the robust information beamforming matrix $\mathbf{W}$ and AN covariance matrix $\mathbf{\Omega}$ are designed by our SRM-1D scheme. Specifically, according to (5), (14), and (17), we maximize the worst-case secrecy rate subject to the total transmit power and the harvested energy constraints. Then the optimization problem can be formulated as

$$
\begin{aligned}
(\mathrm{P1}):\ &\max_{\mathbf{W},\mathbf{\Omega}}\ \bar{R}_s && \text{(20a)}\\
&\text{s.t. } P_s\|\mathbf{W}\mathbf{h}(\theta_{sr})\|^2+\sigma^2\mathrm{Tr}(\mathbf{W}^H\mathbf{W})+\mathrm{Tr}(\mathbf{\Omega})\le P_t, && \text{(20b)}\\
&\quad \rho\big[P_s|\mathbf{h}^H(\theta_{rp})\mathbf{W}\mathbf{h}(\theta_{sr})|^2+\sigma^2\|\mathbf{W}^H\mathbf{h}(\theta_{rp})\|^2\\
&\quad +\mathbf{h}^H(\theta_{rp})\mathbf{\Omega}\mathbf{h}(\theta_{rp})\big]\ge P_{min},\quad \mathbf{\Omega}\succeq\mathbf{0}, && \text{(20c)}
\end{aligned}
$$

where (20b) denotes the total power constraint at the relay, and the first term in (20c) denotes the minimum power required by the ER. We employ a 1D search and a SDR-based algorithm to solve problem (P1). Observe that $\bar{R}_s$ is the difference of two logarithmic functions, which is non-convex and untractable. Similar to [36], we decompose (20) into two sub-problems, yielding:

$$
\begin{aligned}
&\max_{\beta}\ \frac{1}{2}\log_2\left(\frac{1+\phi(\beta)}{1+\beta}\right)\\
&\text{s.t. } 0\le\beta\le\beta_{max},
\end{aligned}
\tag{21}
$$

and

$$
\begin{aligned}
&\phi(\beta)\\
&=\max_{\mathbf{W},\mathbf{\Omega}}\ \frac{P_s|\mathbf{h}^H(\theta_{rd})\mathbf{W}\mathbf{h}(\theta_{sr})|^2}{\sigma^2\|\mathbf{W}^H\mathbf{h}(\theta_{rd})\|^2+\mathbf{h}^H(\theta_{rd})\mathbf{\Omega}\mathbf{h}(\theta_{rd})+\sigma^2}\\
&\text{s.t. } (20b),\ (20c),\\
&\quad\frac{\mathbb{E}_{\Delta\theta_{re_m}}[P_s|\mathbf{h}^H(\theta_{re_m})\mathbf{W}\mathbf{h}(\theta_{sr})|^2]}{\mathbb{E}_{\Delta\theta_{re_m}}[\sigma^2\|\mathbf{W}^H\mathbf{h}(\theta_{re_m})\|^2]+\mathbb{E}[\mathbf{h}^H(\theta_{re_m})\mathbf{\Omega}\mathbf{h}(\theta_{re_m})]+\sigma^2}\\
&\quad\le\beta,\quad m\in\mathcal{M},
\end{aligned}
\tag{22}
$$

where β is a slack variable. The main steps to solve the problem (P1) are as follows. First, for each β inside the interval $[0,\beta_{max}]$, we can obtain a corresponding $\phi(\beta)$ by solving the problem (22). Second, upon substituting β and $\phi(\beta)$ into the objective function of (21), we obtain the secrecy rate corresponding to the given β. Third, we perform a 1D search for β, compare all the secrecy rates obtained and finally we find the optimal value for (21).

As for the above procedure of solving the problem (P1), the most important and complex part is to solve the problem (22) to obtain $\phi(\beta)$. This will be illustrated as follows. Upon defining $\mathbf{w}\triangleq\mathrm{vec}(\mathbf{W})\in\mathbb{C}^{N^2\times1}$, we can rewrite (22) as

$$
\begin{aligned}
\phi(\beta)=v\max_{\mathbf{w},\mathbf{\Omega}}\ &\frac{P_s\mathbf{w}^H\mathbf{A}_1\mathbf{w}}{\sigma^2\mathbf{w}^H\mathbf{A}_2\mathbf{w}+\mathbf{h}^H(\theta_{rd})\mathbf{\Omega}\mathbf{h}(\theta_{rd})+\sigma^2}, && \text{(23a)}\\
\text{s.t. }&\frac{P_s\mathbf{w}^H\mathbf{B}_{1_m}\mathbf{w}}{\sigma^2\mathbf{w}^H\mathbf{B}_{2_m}\mathbf{w}+\mathrm{Tr}(\mathbf{H}_{re_m}\mathbf{\Omega})+\sigma^2}\le\beta,\quad m\in\mathcal{M}, && \text{(23b)}\\
&P_s\mathbf{w}^H\mathbf{C}_1\mathbf{w}+\sigma^2\mathbf{w}^H\mathbf{w}+\mathrm{Tr}(\mathbf{\Omega})\le P_t, && \text{(23c)}\\
&P_s\mathbf{w}^H\mathbf{D}_1\mathbf{w}+\sigma^2\mathbf{w}^H\mathbf{D}_2\mathbf{w}+\mathbf{h}^H(\theta_{rp})\mathbf{\Omega}\mathbf{h}(\theta_{rp})\\
&\ge\frac{P_{min}}{\rho},\quad \mathbf{\Omega}\succeq\mathbf{0}, && \text{(23d)}
\end{aligned}
$$

where

$$
\begin{aligned}
\mathbf{A}_1&=\left[\mathbf{h}^*(\theta_{sr})\mathbf{h}^T(\theta_{sr})\right]\otimes\left[\mathbf{h}(\theta_{rd})\mathbf{h}^H(\theta_{rd})\right], && \text{(24a)}\\
\mathbf{A}_2&=\mathbf{I}_N\otimes\left[\mathbf{h}(\theta_{rd})\mathbf{h}^H(\theta_{rd})\right], && \text{(24b)}\\
\mathbf{B}_{1_m}&=\left[\mathbf{h}^*(\theta_{sr})\mathbf{h}^T(\theta_{sr})\right]\otimes(\mathbf{H}_{re_m}),\quad m\in\mathcal{M}, && \text{(24c)}\\
\mathbf{B}_{2_m}&=\mathbf{I}_N\otimes(\mathbf{H}_{re_m}),m\in\mathcal{M}, && \text{(24d)}\\
\mathbf{C}_1&=\left[\mathbf{h}^*(\theta_{sr})\mathbf{h}^T(\theta_{sr})\right]\otimes\mathbf{I}_N, && \text{(24e)}\\
\mathbf{D}_1&=\left[\mathbf{h}^*(\theta_{sr})\mathbf{h}^T(\theta_{sr})\right]\otimes\left[\mathbf{h}(\theta_{rp})\mathbf{h}^H(\theta_{rp})\right], && \text{(24f)}\\
\mathbf{D}_2&=\mathbf{I}_N\otimes\left[\mathbf{h}(\theta_{rp})\mathbf{h}^H(\theta_{rp})\right]. && \text{(24g)}
\end{aligned}
$$

Given the above vectorization, we show that problem (23) can be transformed into a standard SDP problem. Upon defining $\tilde{\mathbf{W}}\triangleq\mathbf{w}\mathbf{w}^H\in\mathbb{C}^{N^2\times N^2}$, (23) can be rewritten as

$$
\begin{aligned}
\phi(\beta)=\max_{\tilde{\mathbf{W}},\mathbf{\Omega}}\ &\frac{P_s\mathrm{Tr}(\mathbf{A}_1\tilde{\mathbf{W}})}{\sigma^2\mathrm{Tr}(\mathbf{A}_2\tilde{\mathbf{W}})+\mathbf{h}^H(\theta_{rd})\mathbf{\Omega}\mathbf{h}(\theta_{rd})+\sigma^2} && \text{(25a)}\\
\text{s.t. }&P_s\mathrm{Tr}(\mathbf{B}_{1_m}\tilde{\mathbf{W}})-\beta\sigma^2\mathrm{Tr}(\mathbf{B}_{2_m}\tilde{\mathbf{W}})-\beta\mathrm{Tr}(\mathbf{H}_{re_m}\mathbf{\Omega})\\
&\quad-\beta\sigma^2\le0,\quad m\in\mathcal{M}, && \text{(25b)}\\
&P_s\mathrm{Tr}(\mathbf{C}_1\tilde{\mathbf{W}})+\sigma^2\mathrm{Tr}(\tilde{\mathbf{W}})+\mathrm{Tr}(\mathbf{\Omega})\le P_t, && \text{(25c)}\\
&P_s\mathrm{Tr}(\mathbf{D}_1\tilde{\mathbf{W}})+\sigma^2\mathrm{Tr}(\mathbf{D}_2\tilde{\mathbf{W}})+\mathbf{h}^H(\theta_{rp})\mathbf{\Omega}\mathbf{h}(\theta_{rp})\\
&\quad\ge\frac{P_{min}}{\rho}, && \text{(25d)}\\
&\mathrm{rank}(\tilde{\mathbf{W}})=1,\quad \tilde{\mathbf{W}}\succeq\mathbf{0},\ \mathbf{\Omega}\succeq\mathbf{0}. && \text{(25e)}
\end{aligned}
$$

Note that the rank constraint in (25e) is non-convex. By dropping the rank-one constraint in (25e), the SDR of problem (25) can be expressed as

$$
\begin{aligned}
\phi(\beta)=\max_{\tilde{\mathbf{W}},\mathbf{\Omega}}\ &\frac{P_s\mathrm{Tr}(\mathbf{A}_1\tilde{\mathbf{W}})}{\sigma^2\mathrm{Tr}(\mathbf{A}_2\tilde{\mathbf{W}})+\mathbf{h}^H(\theta_{rd})\mathbf{\Omega}\mathbf{h}(\theta_{rd})+\sigma^2}\\
&\text{s.t. } (25b),\ (25c),\ (25d),\quad \tilde{\mathbf{W}}\succeq\mathbf{0},\ \mathbf{\Omega}\succeq\mathbf{0}.
\end{aligned}
\tag{26}
$$

It can be observed that (26) constitutes a quasi-convex problem, which can be transformed into a convex optimization problem by using the Charnes-Cooper transformation [41]. Upon introducing the slack variable τ, problem (26) can be equivalently rewritten as

$$
\begin{aligned}
\phi(\beta)=\max_{\mathbf{Q},\mathbf{\Upsilon},\tau}\ &P_s\mathrm{Tr}(\mathbf{A}_1\mathbf{Q})\\
&\text{s.t. } P_s\mathrm{Tr}(\mathbf{B}_{1_m}\mathbf{Q})-\beta\sigma^2\mathrm{Tr}(\mathbf{B}_{2_m}\mathbf{Q})-\beta\mathrm{Tr}(\bar{\mathbf{H}}_{re_m}\mathbf{\Upsilon})\\
&\quad-\beta\sigma^2\tau\le0,\quad m\in\mathcal{M},\\
&P_s\mathrm{Tr}(\mathbf{C}_1\mathbf{Q})+\sigma^2\mathrm{Tr}(\mathbf{Q})+\mathrm{Tr}(\mathbf{\Upsilon})\le P_t\tau,\\
&\sigma^2\mathrm{Tr}(\mathbf{A}_2\mathbf{Q})+\mathbf{h}^H(\theta_{rd})\mathbf{\Upsilon}\mathbf{h}(\theta_{rd})+\sigma^2\tau=1,\\
&P_s\mathrm{Tr}(\mathbf{D}_1\mathbf{Q})+\sigma^2\mathrm{Tr}(\mathbf{D}_2\mathbf{Q})+\mathbf{h}^H(\theta_{rp})\mathbf{\Upsilon}\mathbf{h}(\theta_{rp})\\
&\quad\ge\frac{P_{min}\tau}{\rho},\quad \mathbf{Q}\succeq\mathbf{0},\ \mathbf{\Upsilon}\succeq\mathbf{0},\ \tau>0,
\end{aligned}
\tag{27}
$$

where $\mathbf{Q}=\tilde{\mathbf{W}}\tau$ and $\mathbf{\Upsilon}=\mathbf{\Omega}\tau$. Since problem (27) is a standard SDP problem [42], its optimal solution can be found by using SDP solvers, such as CVX. If the optimal solution of problem (27) is $(\mathbf{Q}^\star,\mathbf{\Upsilon}^\star,\tau)$, then $(\mathbf{Q}^\star/\tau,\mathbf{\Upsilon}^\star/\tau)$ will be the optimal solution of problem (26).

Since we have dropped the rank-one constraint in the problem (25) and reformulated it as the SDR problem (26), the optimal solution of (26) may not be of rank-one and thus the optimal objective value of (26) generally serves as an upper

bound of (25). Next, we show that the above SDR is in fact tight. We consider the power minimization problem as follows

$$\begin{aligned}&\min_{\tilde{\mathbf{W}},\mathbf{\Omega}} \ P_s\mathrm{Tr}(\mathbf{C}_1\tilde{\mathbf{W}})+\sigma^2\mathrm{Tr}(\tilde{\mathbf{W}})\\ &\text{s.t.} \ \frac{P_s\mathrm{Tr}(\mathbf{A}_1\tilde{\mathbf{W}})}{\sigma^2\mathrm{Tr}(\mathbf{A}_2\tilde{\mathbf{W}})+\mathbf{h}^H(\theta_{rd})\mathbf{\Omega}\mathbf{h}(\theta_{rd})+\sigma^2}\geq\phi(\beta),\\ &\quad (25b),\ (25c),\ (25d),\quad \tilde{\mathbf{W}}\succeq\mathbf{0},\ \mathbf{\Omega}\succeq\mathbf{0},\end{aligned}\tag{28}$$

where $\phi(\beta)$ is the optimal value of problem (26). Observe that the optimal solution of problem (28) is also an optimal solution of (26). The proof is similar to that in [35] and thus omitted here for brevity. In order to obtain the optimal solution of (25), we should first obtain the optimal solution $(\tilde{\mathbf{W}}^\star,\mathbf{\Omega}^\star)$ and the optimal value $\phi(\beta)$ of problem (26) by solving (27). If $\mathrm{rank}(\tilde{\mathbf{W}}^\star)=1$, then we get the optimal solution of (25). Otherwise, the rank-one solution can be found by solving (28).

Lemma 1: The optimal solution $\tilde{\mathbf{W}}^\star$ in (28) satisfies $\mathrm{rank}(\tilde{\mathbf{W}}^\star)=1$.

Proof: See Appendix B. ∎

Since $\tilde{\mathbf{W}}^\star$ is a rank-one matrix, we can write $\tilde{\mathbf{W}}^\star=\mathbf{w}^\star\mathbf{w}^{\star H}$ by using eigenvalue decomposition. Thus, the SDR is tight and the optimal solution of (23) is $\mathbf{w}^\star$ and $\mathbf{\Omega}^\star$. Up to now, we have solved the problem (22).

Let us now return to the procedure used for the problem (21). The maximum of β should be found by 1D search. According to the fact that the secrecy rate is always greater than or equal to zero, we get

$$\begin{aligned}\beta&\leq\frac{P_s\mathbf{w}^H\mathbf{A}_1\mathbf{w}}{\sigma^2\mathbf{w}^H\mathbf{A}_2\mathbf{w}+\mathbf{h}^H(\theta_{rd})\mathbf{\Omega}\mathbf{h}(\theta_{rd})+\sigma^2}\\ &\leq\frac{P_s\mathbf{w}^H\mathbf{A}_1\mathbf{w}}{\sigma^2\mathbf{w}^H\mathbf{A}_2\mathbf{w}+\sigma^2}.\end{aligned}\tag{29}$$

From the transmit power constraint in (23), we have $\frac{\sigma^2}{P_t}\mathbf{w}^H\mathbf{w}\leq 1$, hence

$$\beta\leq\frac{P_s\mathbf{w}^H\mathbf{A}_1\mathbf{w}}{\sigma^2\mathbf{w}^H\mathbf{A}_2\mathbf{w}+\frac{\sigma^4}{P_t}\mathbf{w}^H\mathbf{w}}=\frac{P_s\mathbf{w}^H\mathbf{A}_1\mathbf{w}}{\mathbf{w}^H(\sigma^2\mathbf{A}_2+\frac{\sigma^4}{P_t}\mathbf{I}_{N^2})\mathbf{w}}.\tag{30}$$

Observe that $\mathbf{A}_1$ can be recast as

$$\mathbf{A}_1=[\mathbf{h}^*(\theta_{sr})\otimes\mathbf{h}(\theta_{rd})]\left[\mathbf{h}^T(\theta_{sr})\otimes\mathbf{h}^H(\theta_{rd})\right]=\mathbf{a}_1\mathbf{a}_1^H,\tag{31}$$

where $\mathbf{a}_1\in\mathbb{C}^{N^2\times 1}$. Therefore, we have $\mathrm{rank}(\mathbf{A}_1)=1$. According to (30) and (31), the upper bound of β is given by

$$\beta\leq P_s\mathbf{a}_1^H(\sigma^2\mathbf{A}_2+\frac{\sigma^4}{P_t}\mathbf{I}_{N^2})^{-1}\mathbf{a}_1=\beta_{max}.\tag{32}$$

The proposed SRM-1D scheme is summarized in Algorithm 1.

Algorithm 1 Maximize Secrecy Rate Based on 1D Search

Initialize ε, n, β, and compute β_{max}.
repeat
1) Set $n=n+1$, $\beta=\beta+\varepsilon$.
2) Solve problem (27) and obtain the optimal solution $(\tilde{\mathbf{Q}}^\star(n),\mathbf{\Upsilon}^\star(n),\tau^\star(n))$ and optimal value $\phi(\beta)(n)$.
3) Compute secrecy rate $R_s(n)$ according to the objective function of (21).

until $\beta>\beta_{max}$.
• $n=\arg\max_n Rs(n)$, and $\tilde{\mathbf{W}}^\star=\mathbf{Q}^\star(n)/\tau^\star(n)$, $\mathbf{\Omega}^\star=\tilde{\mathbf{\Upsilon}}^\star(n)/\tau^\star(n)$. If rank($\tilde{\mathbf{W}}^\star$) = 1, then go to next step; otherwise, solve (28).
• By using eigenvalue decomposition, we can obtain $\mathbf{w}^\star$, and reconstruct $\mathbf{W}^\star$; $\mathbf{z}=\mathbf{\Omega}^{\star\frac{1}{2}}\mathbf{v}$ and $\mathbf{v}\sim\mathcal{CN}(0,\mathbf{I}_N)$.
return $\mathbf{W}^\star$ and $\mathbf{z}^\star$.

B. Maximization of Signal-to-Leakage-AN-Noise-Ratio (Max-SLANR) Scheme

In the previous subsection, we employed a 1D search and a SDR-based algorithm to solve problem (P1). Although we have already derived β_{max}, for limiting the range of the 1D search, the complexity of the 1D search still remains high, since for each β, a SDP with $\mathcal{O}(N^{13})$ (as can be proved later in (53)) has to be solved. In order to avoid employing the 1D search, we propose an alternative algorithm for the suboptimal solution of (P1). Specifically, we propose an algorithm for maximizing the SLANR rather than the secrecy rate, subject to the total power and to the harvested energy constraints. Based on the concept of leakage [43], from (6) and (8), the optimization problem (P1) can be reformulated as (33), shown at the top of the next page. The numerator of the objective function in (33) represents the received confidential message power at the IR, and the first term in the denominator denotes the sum of confidential message power leaked to all eavesdroppers.

Following similar steps as in Section III-A and dropping the rank-one constraint, the related SDR problem can be formulated as (34), shown at the top of the next page, where $\tilde{\mathbf{W}}=\mathbf{w}\mathbf{w}^H\in\mathbb{C}^{N^2\times N^2}$ and $\mathbf{w}=\mathrm{vec}(\mathbf{W})\in\mathbb{C}^{N^2\times 1}$. Note that all constraints in (34) are convex. However, the objective function is a linear fractional function, which is quasi-convex. Similar to (26), we transform (34) into a convex optimization problem by using the Charnes-Cooper transformation [41]. Problem (34) can then be equivalently rewritten as

$$\begin{aligned}&\max_{\mathbf{Q},\mathbf{\Upsilon},\tau} \ P_s\mathrm{Tr}(\mathbf{A}_1\mathbf{Q})\\ &\text{s.t.} \ \sum_{m=1}^{M}P_s\mathrm{Tr}(\mathbf{B}_{1_m}\mathbf{Q})+\mathbf{h}^H(\theta_{rd})\mathbf{\Upsilon}\mathbf{h}(\theta_{rd})\\ &\quad+\sigma^2\mathrm{Tr}(\mathbf{A}_2\mathbf{Q})+\sigma^2\tau=1,\\ &\quad P_s\mathrm{Tr}(\mathbf{C}_1\mathbf{Q})+\sigma^2\mathrm{Tr}(\mathbf{Q})+\mathrm{Tr}(\mathbf{\Upsilon})\leq P_t\tau,\\ &\quad P_s\mathrm{Tr}(\mathbf{D}_1\mathbf{Q})+\sigma^2\mathrm{Tr}(\mathbf{D}_2\mathbf{Q})+\mathbf{h}^H(\theta_{rp})\mathbf{\Upsilon}\mathbf{h}(\theta_{rp})\\ &\quad\geq\frac{P_{min}\tau}{\rho},\quad\mathbf{Q}\succeq\mathbf{0},\ \mathbf{\Upsilon}\succeq\mathbf{0},\ \tau>0,\end{aligned}\tag{35}$$

where τ is a slack variable, $\mathbf{Q}=\tilde{\mathbf{W}}\tau$ and $\mathbf{\Upsilon}=\mathbf{\Omega}\tau$. To prove that the relaxation is tight, we consider the associated power minimization problem, which is similar to that in Section III-A, yielding

$$\begin{aligned}&\min_{\tilde{\mathbf{W}},\mathbf{\Omega}} \ P_s\mathrm{Tr}(\mathbf{C}_1\tilde{\mathbf{W}})+\sigma^2\mathrm{Tr}(\tilde{\mathbf{W}})\\ &\text{s.t.} \ -P_s\mathrm{Tr}(\mathbf{A}_1\tilde{\mathbf{W}})+\phi\sum_{m=1}^{M}P_s\mathrm{Tr}(\mathbf{B}_{1_m}\tilde{\mathbf{W}})+\\ &\quad\phi\mathbf{h}^H(\theta_{rd})\mathbf{\Omega}\mathbf{h}(\theta_{rd})+\phi\sigma^2\mathrm{Tr}(\mathbf{A}_2\tilde{\mathbf{W}})+\phi\sigma^2\leq 0,\\ &\quad P_s\mathrm{Tr}(\mathbf{C}_1\tilde{\mathbf{W}})+\sigma^2\mathrm{Tr}(\tilde{\mathbf{W}})+\mathrm{Tr}(\mathbf{\Omega})\leq P_t,\\ &\quad P_s\mathrm{Tr}(\mathbf{D}_1\tilde{\mathbf{W}})+\sigma^2\mathrm{Tr}(\mathbf{D}_2\tilde{\mathbf{W}})+\mathbf{h}^H(\theta_{rp})\mathbf{\Omega}\mathbf{h}(\theta_{rp})\\ &\quad\geq\frac{P_{min}}{\rho},\quad\mathbf{\Omega}\succeq\mathbf{0},\ \tilde{\mathbf{W}}\succeq\mathbf{0},\end{aligned}\tag{36}$$

$$\max_{\mathbf{W},\mathbf{\Omega}} \frac{P_s|\mathbf{h}^H(\theta_{rd})\mathbf{W}\mathbf{h}(\theta_{sr})|^2}{\sum_{m=1}^{M}\mathbb{E}_{\Delta\theta_{re_m}}[P_s|\mathbf{h}^H(\theta_{re_m})\mathbf{W}\mathbf{h}(\theta_{sr})|^2]+\mathbf{h}^H(\theta_{rd})\mathbf{\Omega}\mathbf{h}(\theta_{rd})+\sigma^2\|\mathbf{W}^H\mathbf{h}(\theta_{rd})\|^2+\sigma^2}$$
$$\text{s.t. } P_s\|\mathbf{W}\mathbf{h}(\theta_{sr})\|^2+\sigma^2\mathrm{Tr}(\mathbf{W}^H\mathbf{W})+\mathrm{Tr}(\mathbf{\Omega})\le P_t,$$
$$P_s|\mathbf{h}^H(\theta_{rp})\mathbf{W}\mathbf{h}(\theta_{sr})|^2+\sigma^2\|\mathbf{W}^H\mathbf{h}(\theta_{rp})\|^2+\mathbf{h}^H(\theta_{rp})\mathbf{\Omega}\mathbf{h}(\theta_{rp})\ge\frac{P_{min}}{\rho},\quad \mathbf{\Omega}\succeq\mathbf{0}. \tag{33}$$

$$\max_{\tilde{\mathbf{W}},\mathbf{\Omega}} \frac{P_s\mathrm{Tr}(\mathbf{A}_1\tilde{\mathbf{W}})}{\sum_{m=1}^{M}P_s\mathrm{Tr}(\mathbf{B}_{1_m}\tilde{\mathbf{W}})+\mathbf{h}^H(\theta_{rd})\mathbf{\Omega}\mathbf{h}(\theta_{rd})+\sigma^2\mathrm{Tr}(\mathbf{A}_2\tilde{\mathbf{W}})+\sigma^2}$$
$$\text{s.t. } P_s\mathrm{Tr}(\mathbf{C}_1\tilde{\mathbf{W}})+\sigma^2\mathrm{Tr}(\tilde{\mathbf{W}})+\mathrm{Tr}(\mathbf{\Omega})\le P_t,$$
$$P_s\mathrm{Tr}(\mathbf{D}_1\tilde{\mathbf{W}})+\sigma^2\mathrm{Tr}(\mathbf{D}_2\tilde{\mathbf{W}})+\mathbf{h}^H(\theta_{rp})\mathbf{\Omega}\mathbf{h}(\theta_{rp})\ge\frac{P_{min}}{\rho},\tilde{\mathbf{W}}\succeq\mathbf{0},\quad\mathbf{\Omega}\succeq\mathbf{0}. \tag{34}$$

where ϕ is the optimal value of (35). Problem (36) is a standard SDP problem.

Lemma 2: The optimal solution $\tilde{\mathbf{W}}^\star$ in (36) satisfies $\mathrm{rank}(\tilde{\mathbf{W}}^\star)=1$.

Proof: See Appendix C. ∎

C. Low-Complexity SCA Scheme

In Sections III-A and III-B, we have proposed the SRM-1D and the Max-SLANR schemes to obtain the information beamforming matrix and the AN covariance matrix. Both of the two schemes have high computational complexity, because their optimization variables are matrices. To facilitate implementation in practice, in this subsection, we propose a low complexity scheme based on SCA. Specifically, we first formulate the optimization problem, then convert it into the SOCP problem, and use the SCA method to solve the problem iteratively. In contrast to designing the AN covariance matrix $\mathbf{\Omega}$ as in the previous two subsections, here we are devoted to designing the AN beamforming vector $\mathbf{v}$, where $\mathbf{\Omega}=\mathbf{v}\mathbf{v}^H$.

The optimization problem (20) can be rewritten as

$$\max_{\mathbf{w},\mathbf{v}}\min_{m}\ \frac{1+\mathrm{SINR}_d}{1+\mathbb{E}_{\Delta\theta_{re_m}}[\mathrm{SINR}_{e_m}]} \tag{37a}$$
$$\text{s.t. } \mathbf{w}^H(P_s\mathbf{C}_1+\sigma^2\mathbf{I}_{N^2})\mathbf{w}+\mathbf{v}^H\mathbf{v}\le P_t, \tag{37b}$$
$$\mathbf{w}^H(P_s\mathbf{D}_1+\sigma^2\mathbf{D}_2)\mathbf{w}+\mathbf{v}^H\mathbf{h}(\theta_{rp})\mathbf{h}^H(\theta_{rp})\mathbf{v}\ge\frac{P_{min}}{\rho}, \tag{37c}$$

where SINR_d and $\mathbb{E}[\mathrm{SINR}_{e_m}]$ are defined in (23a) and (23b), respectively. By introducing the slack variables r_1 and r_2, problem (37) is equivalently rewritten as

$$\max_{\mathbf{w},\mathbf{v},r_1,r_2}\ r_1r_2 \tag{38a}$$
$$\text{s.t. } 1+\mathrm{SINR}_d\ge r_1, \tag{38b}$$
$$1+\mathbb{E}_{\Delta\theta_{re_m}}[\mathrm{SINR}_{e_m}]\le\frac{1}{r_2},\quad m\in\mathcal{M}, \tag{38c}$$
$$(37b),\ (37c). \tag{38d}$$

(38b) and (38c) can be rearranged as

$$\sigma^2\mathbf{w}^H\mathbf{A}_2\mathbf{w}+\mathbf{v}^H\mathbf{h}(\theta_{rd})\mathbf{h}^H(\theta_{rd})\mathbf{v}+\sigma^2\le\frac{P_s\mathbf{w}^H\mathbf{A}_1\mathbf{w}}{r_1-1}, \tag{39a}$$
$$\mathbf{w}^H(P_s\mathbf{B}_{1_m}+\sigma^2\mathbf{B}_{2_m})\mathbf{w}+\mathbf{v}^H\mathbf{H}_{re_m}\mathbf{v}+\sigma^2\le\frac{1}{r_2}(\sigma^2\mathbf{w}^H\mathbf{B}_{2_m}\mathbf{w}+\mathbf{v}^H\mathbf{H}_{re_m}\mathbf{v}+\sigma^2),m\in\mathcal{M}, \tag{39b}$$

respectively. Since the quadratic-over-linear function is convex [42], the right-hand-side (RHS) expressions of (39a) and (39b) are convex functions ($r_1>1,r_2>0$). In the following, we first transform (39a) and (39b) into convex constraints by using the first-order Talyor expansions [44], and then convert them into the second-order cone (SOC) constraints. To this end, we define

$$f_{\mathbf{A},a}(\mathbf{x},r)=\frac{\mathbf{x}^H\mathbf{A}\mathbf{x}}{r-a}, \tag{40}$$

where $\mathbf{A}\succeq\mathbf{0}$ and $r>a$. We perform the first-order Taylor expansion of (40) at point $(\tilde{\mathbf{x}},\tilde{r})$ [20], yielding:

$$f_{\mathbf{A},a}(\mathbf{x},r)\ge F_{\mathbf{A},a}(\mathbf{x},r,\tilde{\mathbf{x}},\tilde{r})=\frac{2\mathrm{Re}\{\tilde{\mathbf{x}}^H\mathbf{A}\mathbf{x}\}}{\tilde{r}-a}-\frac{\tilde{\mathbf{x}}^H\mathbf{A}\tilde{\mathbf{x}}}{(\tilde{r}-a)^2}(r-a), \tag{41}$$

where the inequality holds due to the convexity of $f_{\mathbf{A},a}(\mathbf{x},r)$ with respect to $\mathbf{x}$ and r. Therefore, (39a) and (39b) can be rewritten as

$$\sigma^2\mathbf{w}^H\mathbf{A}_2\mathbf{w}+\mathbf{v}^H\mathbf{h}(\theta_{rd})\mathbf{h}^H(\theta_{rd})\mathbf{v}+\sigma^2\le P_sF_{\mathbf{A}_1,1}(\mathbf{w},r_1,\tilde{\mathbf{w}},\tilde{r}_1), \tag{42a}$$
$$\mathbf{w}^H(P_s\mathbf{B}_{1_m}+\sigma^2\mathbf{B}_{2_m})\mathbf{w}+\mathbf{v}^H\mathbf{H}_{re_m}\mathbf{v}+\sigma^2\le\mathfrak{F}_m,\quad m\in\mathcal{M}, \tag{42b}$$

which can be transformed into the SOC constraints, i.e.,

$$\left\|\left[2\sigma\mathbf{A}_2^{\frac{1}{2}}\mathbf{w};2\mathbf{h}^H(\theta_{rd})\mathbf{v};2\sigma;P_sF_{\mathbf{A}_1,1}(\mathbf{w},r_1,\tilde{\mathbf{w}},\tilde{r}_1)-1\right]\right\|\le P_sF_{\mathbf{A}_1,1}(\mathbf{w},r_1,\tilde{\mathbf{w}},\tilde{r}_1)+1, \tag{43a}$$
$$\left\|\left[2(P_s\mathbf{B}_{1_m}+\sigma^2\mathbf{B}_{2_m})^{\frac{1}{2}}\mathbf{w};2\mathbf{H}_{re_m}^{\frac{1}{2}}\mathbf{v};2\sigma;\mathfrak{F}_m-1\right]\right\|\le\mathfrak{F}_m+1,\quad m\in\mathcal{M}, \tag{43b}$$

where $\mathfrak{F}_m$ is defined as

$$\mathfrak{F}_m=\sigma^2F_{\mathbf{B}_{2_m},0}(\mathbf{w},r_2,\tilde{\mathbf{w}},\tilde{r}_2)+F_{\mathbf{H}_{re_m},0}(\mathbf{v},r_2,\tilde{\mathbf{v}},\tilde{r}_2)+\sigma^2\left(\frac{2}{\tilde{r}_2}-\frac{r_2}{\tilde{r}_2^2}\right). \tag{44}$$

It is easy to see that the objective function of the problem (38) is non-concave and the constraint (37c) is non-convex. To handle the non-concave objective function, we introduce the slack variables t and ψ and then rewrite the

problem (38) as

$$\max_{\mathbf{w},\mathbf{v},r_1,r_2,t,\psi} \quad t \tag{45a}$$

$$\text{s.t. } r_1 r_2 \geq \psi^2, \quad \psi^2 \geq t, \tag{45b}$$

$$(43a),\ (43b),\ (37b),\ (37c). \tag{45c}$$

Note that the first term of (45b) can be rearranged as the SOC constraint, i.e.,

$$\|[r_1 - r_2; 2\psi]\| \leq r_1 + r_2. \tag{46}$$

For the second term of the (45b), we employ the first-order Taylor expansion at the point $\tilde{\psi}$ and transform it into the linear constraint, i.e.,

$$2\tilde{\psi}\psi - \tilde{\psi}^2 \geq t. \tag{47}$$

In the following, we will focus on dealing with the non-convex constraint (37c). To convert (37c) into a convex constraint, we define

$$u_{\mathbf{A}}(\mathbf{x}) = \mathbf{x}^H \mathbf{A}\mathbf{x}, \tag{48}$$

where $\mathbf{A} \succeq \mathbf{0}$. Since $u_{\mathbf{A}}(\mathbf{x})$ is a convex function, we have the following inequality

$$u_{\mathbf{A}}(\mathbf{x}) \geq U_{\mathbf{A}}(\mathbf{x}, \tilde{\mathbf{x}}) = 2\mathrm{Re}(\tilde{\mathbf{x}}^H \mathbf{A}\mathbf{x}) - \tilde{\mathbf{x}}^H \mathbf{A}\tilde{\mathbf{x}}, \tag{49}$$

where the inequality (49) holds based on the first-order Taylor expansion at the point $\tilde{\mathbf{x}}$. According to (49), (37c) can be rewritten as

$$U_{\mathbf{G}}(\mathbf{w}, \tilde{\mathbf{w}}) + U_{\mathbf{H}_{rp}}(\mathbf{v}, \tilde{\mathbf{v}}) \geq \frac{P_{min}}{\rho}, \tag{50}$$

where $\mathbf{G} = P_s\mathbf{D}_1 + \sigma^2\mathbf{D}_2$ and $\mathbf{H}_{rp} = \mathbf{h}(\theta_{rp})\mathbf{h}^H(\theta_{rp})$. In addition, (37b) can be equivalently rewritten as

$$\left\| \left[(P_s\mathbf{C}_1 + \sigma^2\mathbf{I}_{N^2})^{\frac{1}{2}}\mathbf{w}; \mathbf{v} \right] \right\| \leq \sqrt{P_t}. \tag{51}$$

According to the above transformation of the objective function and the constraints of problem (37), we can convert (37) into the following SOCP problem

$$\max_{\mathbf{w},\mathbf{v},r_1,r_2,t,\psi} \quad t$$

$$\text{s.t. } (46),\ (47),\ (50),\ (51),\ (43a),\ (43b). \tag{52}$$

It can be seen that the optimization problem (52) consists of a linear objective function and several SOC constraints. Therefore, problem (52) is a convex optimization problem. For a given feasible solution $(\tilde{\mathbf{w}}, \tilde{\mathbf{v}}, \tilde{r}_1, \tilde{r}_2, \tilde{\psi})$, we can solve the problem (52) by means of convex optimization tools such as CVX [42]. Based on the idea of SCA, the original optimization problem (37) can be solved iteratively by solving a series of convex subproblems (52). The current optimal solution of the convex subproblem (52) is gradually approaching the optimal solution of the original problem with the increase of the number of iterations, until the algorithm converges [45]. Algorithm 2 lists the detailed process of the SCA algorithm.

Algorithm 2 SCA Algorithm for Solving Problem (37)

Initialize: Given a feasible solution $(\tilde{\mathbf{w}}^0, \tilde{\mathbf{v}}^0, \tilde{r}_1^0, \tilde{r}_2^0, \tilde{\psi}^0)$; n=0.
repeat
1. Solve the problem (52) with $(\tilde{\mathbf{w}}^n, \tilde{\mathbf{v}}^n, \tilde{r}_1^n, \tilde{r}_2^n, \tilde{\psi}^n)$ and obtain the current optimal solution $(\tilde{\mathbf{w}}^*, \tilde{\mathbf{v}}^*, \tilde{r}_1^*, \tilde{r}_2^*, \tilde{\psi}^*)$; n=n+1.
2. Update $(\tilde{\mathbf{w}}^n, \tilde{\mathbf{v}}^n, \tilde{r}_1^n, \tilde{r}_2^n, \tilde{\psi}^n)$=$(\tilde{\mathbf{w}}^*, \tilde{\mathbf{v}}^*, \tilde{r}_1^*, \tilde{r}_2^*, \tilde{\psi}^*)$.
3. Compute secrecy rate $\bar{R}_s^n$.
until $|\bar{R}_s^n - \bar{R}_s^{n-1}| < \delta$ is met, where δ denotes the convergence tolerance.

D. Complexity Analysis

In this section, we analyze and compare the complexity of the three schemes proposed in the previous three subsections. For the SRM-1D scheme, we convert the SRM problem to the SDP form and solve it with an 1D search. The complexity of each search is calculated according to problem (27). Problem (27) consists of $M + 5$ linear constraints with dimension 1, one LMI constraint of size N^2, and one LMI constraint of size N. The number of decision variables n is on the order of $N^4 + N^2 + 1$. Therefore, the total complexity based on the SRM-1D scheme can be expressed as [46]

$$\mathcal{O}\Big(nT\sqrt{N^2+N+M+5}\big(N^6+N^3+n(N^4+N^2 + M+5)+M+5+n^2\big)\ln(1/\epsilon)\Big), \tag{53}$$

where T denotes the number of iterations in the 1D search and ϵ denotes the computation accuracy.

For the Max-SLANR scheme, we compute the complexity of the optimization problem (35), which consists of one LMI constraint with size of N^2, one LMI constraint with size of N and five linear constraints. The number of decision variables n is on the order of N^4+N^2+1. Therefore, the total complexity based on the Max-SLANR scheme can be expressed as

$$\mathcal{O}\Big(n\sqrt{N^2+N+5}\big(N^6+N^3+n(N^4+N^2+5) + 5+n^2\big)\ln(1/\epsilon)\Big). \tag{54}$$

For the proposed SCA scheme, we first formulate the SRM problem, then convert it into the SOCP form, and use the SCA algorithm to solve it iteratively. The complexity of each iteration is calculated according to problem (52). Problem (52) includes two linear constraints, one SOC constraint of dimension 2, one SOC constraint of dimension $N^2 + N$, M+1 SOC constraints of dimension N^2+N+1. The number of decision variables n is on the order of N^2+N+4. Therefore, the total complexity based on the SCA scheme is given by

$$\mathcal{O}\Big(nL\sqrt{2M+8}\big((N^2+N)^2+(M+1)(N^2+N+1)^2 + 6+2n+n^2\big)\ln(1/\epsilon)\Big), \tag{55}$$

where L is the number of iterations. The complexity of the proposed algorithms is also listed in Table I at the top the next page.

Discussions: Upon comparing (53), (54) and (55), it can be observed that the complexity of the SCA algorithm is much

TABLE I
COMPLEXITY ANALYSIS OF PROPOSED ALGORITHMS

Algorithms	Complexity order $\big($suppressing $\ln(\frac{1}{\epsilon})\big)$
SRM-1D-Robust	$\mathcal{O}\Big(nT\sqrt{N^2+N+M+5}\big(N^6+N^3+n(N^4+N^2+M+5)+M+5+n^2\big)\Big)$, where $n=\mathcal{O}(N^4+N^2+1)$.
Max-SLANR-Robust	$\mathcal{O}\Big(n\sqrt{N^2+N+5}\big(N^6+N^3+n(N^4+N^2+5)+5+n^2\big)\Big)$, where $n=\mathcal{O}(N^4+N^2+1)$.
SCA-Robust	$\mathcal{O}\Big(nL\sqrt{2M+8}\big((N^2+N)^2+(M+1)(N^2+N+1)^2+6+2n+n^2\big)\Big)$, where $n=\mathcal{O}(N^2+N+4)$.

lower than that of the SRM-1D and the Max-SLANR schemes. The complexity of the Max-SLANR scheme is slightly lower than that of the SRM-1D scheme, but the SLANR scheme does not require 1D search. Moreover, the complexity of the SRM-1D scheme grows linearly upon increasing the precision of the 1D search, with the number of iterations T, and it grows with the number M of eavesdroppers, while the complexity of the Max-SLANR scheme is not related to either of them. This implies that when the number of eavesdroppers increases, the complexity of the Max-SLANR scheme remains constant, while the complexity of the SRM-1D and SCA schemes increases. For example, for a system with $N=6$, $M=2$, $T=12$ and $L=6$, the complexity of the SRM-1D, the Max-SLANR, and SCA schemes, is $\mathcal{O}(3.98\times10^{11})$, $\mathcal{O}(3.25\times10^{10})$, and $\mathcal{O}(8.87\times10^{6})$, respectively. Therefore, the complexity of the SCA scheme is much lower than that of the other two schemes.

IV. SIMULATION RESULTS

In this section, we evaluate the performance of our SRM-1D, Max-SLANR, and SCA schemes by Monte Carlo simulations. Furthermore, we develop a method based on ZF [25] to show the superiority of our schemes. Additionally, since in our proposed scheme, we take into account the estimation error of the direction angles of the eavesdroppers at the relay, we also consider the scenario relying on perfect estimation of the direction angle of eavesdroppers from the relay for arriving at a performance upper-bound of our schemes.

In the following, we denote by 'SRM-1D-Perfect' and 'SRM-1D-Robust' the SRM-1D method with perfect and imperfect knowledge of the direction angles from the relay to the eavesdroppers, respectively, and represent by 'SCA-Robust' and 'SLANR-Robust' our SCA and Max-SLANR schemes, respectively, when taking into consideration the estimation error of direction angles at the relay. The simulation parameters are listed in Table II, unless otherwise stated. The free-space path loss model used is defined as

$$g_{mn}=\left(\frac{d_{mn}}{d_0}\right)^{-2}, \tag{56}$$

where g_{mn} and d_{mn} denote the path loss and distance between node m and node n, while d_0 is the reference distance, which is set to 10m. The distances from the relay to other nodes (source, IR, ER and eavesdroppers) are assumed to be the same, which are set to 80 meters, i.e., $g_{mn}=\frac{1}{64}$. The direction angles of the source, IR, ER and eavesdroppers are $\theta_{sr}=-\frac{7\pi}{18}$, $\theta_{rd}=\frac{\pi}{2}$, $\theta_{rp}=\frac{\pi}{4}$ and $\{\theta_{re_1},\theta_{re_2}\}=\{\frac{\pi}{3},\frac{11\pi}{18}\}$, respectively. The location of the source, relay, IR, ER and eavesdroppers in the Cartesian coordinate system is shown in Fig. 2.[1]

TABLE II
SIMULATION PARAMETER

Parameters	Values
Transmit power at the relay (P_t)	30dBm
Transmit power at the source (P_s)	30dBm
Noise variance (σ^2)	-10dBm
Number of transmit antennas at the relay (N)	6
Number of eavesdroppers (M)	2
Minimum energy required by the ER (P_{min})	10dBm
Maximum angle estimation error ($\triangle\theta_{\max}$)	6°
Normalization factor (K_e)	0.9
Energy transfer efficiency (ρ)	0.8
Direction angle of the source (θ_{sr})	$-\frac{7\pi}{18}$
Direction angle of the IR (θ_{rd})	$\frac{\pi}{2}$
Direction angle of the eavesdroppers ($\theta_{re_1},\theta_{re_2}$)	$\frac{\pi}{3}$, $\frac{11\pi}{18}$
Convergence tolerance (δ)	10^{-4}

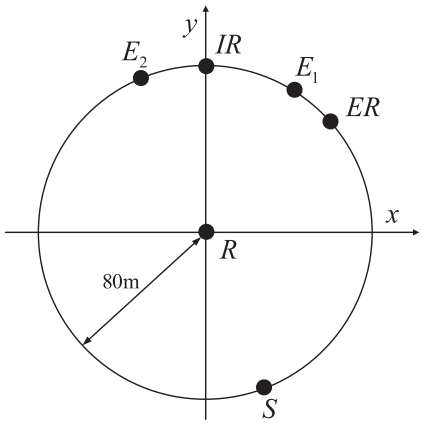

Fig. 2. The location of source, relay, IR, ER and eavesdroppers.

iIn Fig. 3, we show the secrecy rate versus the total power P_t at the relay. Firstly, it can be observed that the secrecy rate grows upon increasing the transmit power P_t at the relay for all cases. Secondly, compared to other schemes, SRM-1D-Perfect scheme has the best secrecy rate, because it has perfectly obtain the eavesdroppers' directional angle information. Thirdly, the proposed SRM-1D-Robust slightly outperforms the proposed SLANR-Robust arrangement. For example, when $P_t=30\mathrm{dBm}$, the secrecy rate of the Max-SLANR-Robust scheme is 0.05bits/s/Hz lower than that of the SRM-1D-Robust scheme. This is because the

[1]Note that all nodes in Fig. 2 can also be distributed to other locations around the circle. Here we just provide a setup case to evaluate the performance of the proposed schemes.

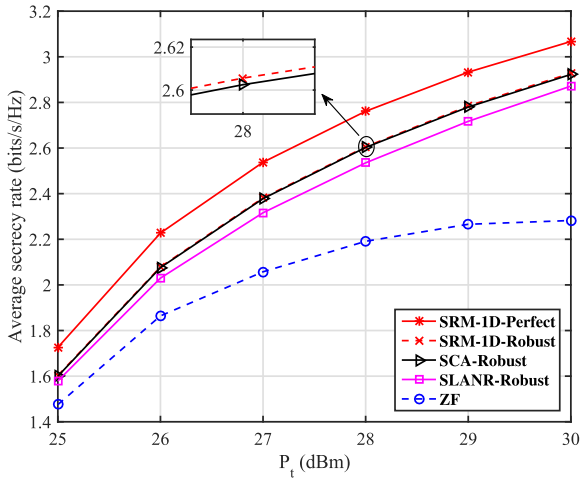

Fig. 3. Average secrecy rate versus the transmit power at relay for $N = 6$, $M = 2$, $P_s = 30\text{dBm}$, $P_{\min} = 5\text{dBm}$, $\Delta\theta_{\max} = 6°$.

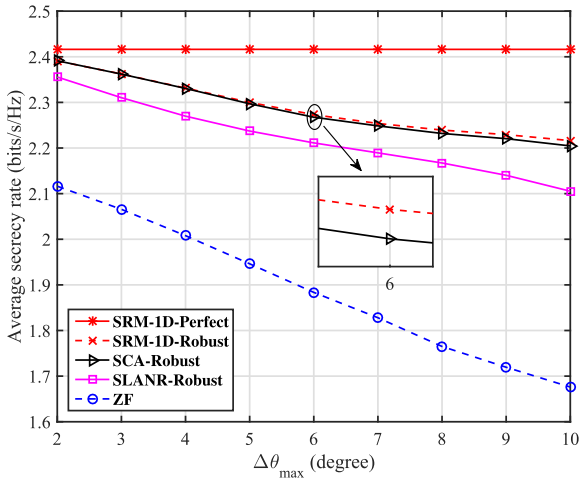

Fig. 5. Average secrecy rate versus the maximum estimate error angle for $N = 6$, $M = 2$, $P_s = 30\text{dBm}$, $P_t = 30\text{dBm}$, $P_{\min} = 10\text{dBm}$.

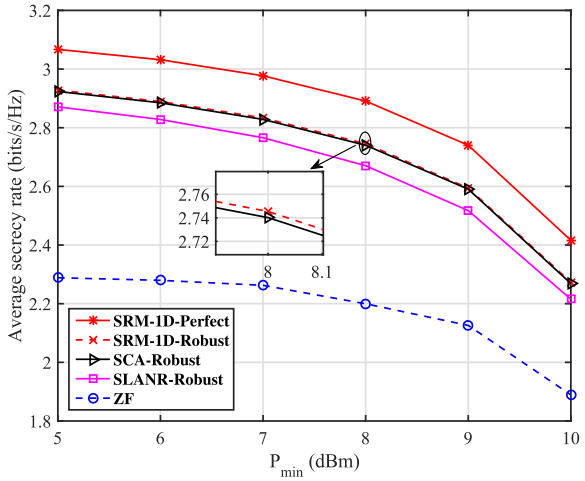

Fig. 4. Average secrecy rate versus the minimum energy required by the ER for $N = 6$, $M = 2$, $P_s = 30\text{dBm}$, $P_t = 30\text{dBm}$, $\Delta\theta_{\max} = 6°$.

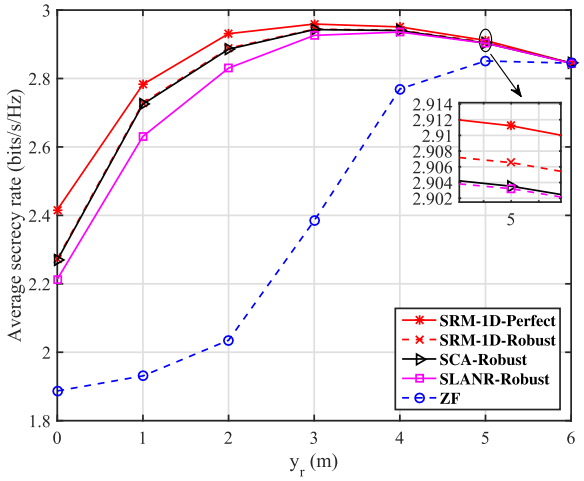

Fig. 6. Average secrecy rate versus the location of relay for $N = 6$, $M = 2$, $P_s = 30\text{dBm}$, $P_t = 30\text{dBm}$, $P_{\min} = 10\text{dBm}$, $\Delta\theta_{\max} = 6°$.

SRM-1D-Robust scheme is the optimal solution, while the SLANR-Robust scheme is a suboptimal solution. Fourthly, the secrecy rate of SCA-Robust scheme is very close to that of the SRM-1D-Robust scheme. However, the complexity of the SCA-Robust scheme is much lower than that of the SRM-1D-Robust scheme. Finally, compared to the ZF scheme, our schemes provide significant performance improvements.

Fig. 4 shows the secrecy rate versus the minimum energy required by the ER for $N = 6$, $P_s = 30\text{dBm}$, $P_t = 30\text{dBm}$, $\Delta\theta = 6°$. Naturally, the secrecy rate decreases with the increase of the minimum energy required by the ER for all cases. The reason behind this is that the more power is used for energy harvesting, the less power remains for secure communication, when the transmit power at the relay is fixed. Furthermore, when $P_{\min} < 9\text{dBm}$, it is observed that the secrecy rate decreases slowly. But when $P_{\min} > 9\text{dBm}$, the secrecy rate decreases rapidly. This is because the signal is transmitted over 80m away from the relay, hence the power of the signal is only 12dBm due to the path loss. Since the energy transfer efficiency is $\rho = 0.8$ and $P_{\min} > 9\text{dBm}$, the power of the transmit signal is mainly used for satisfying the energy harvesting constraint, which results in a rapid reduction of the secrecy rate for all the schemes.

In Fig. 5, by fixing $P_t = 30\text{dBm}$ and $P_{\min} = 10\text{dBm}$, we investigate the effect of the maximum angular estimation error $\Delta\theta_{\max}$ of the eavesdroppers on the secrecy rate. The SRM-1D-Perfect curve remains constant for all $\Delta\theta_{\max}$ values and outperforms the other schemes due to the perfect knowledge of the directional angle. With the increase of $\Delta\theta_{\max}$, the secrecy rates achieved by our robust schemes degrades slowly, because the proposed algorithms have considered the statistical property of the estimation error. As such, they are robust against the effects of estimation errors.

Fig. 6 shows the secrecy rate versus the location of the relay. We denote the coordinates of the relay by (x_r, y_r). In this simulation, we fix x_r to zero and assume that the relay moves vertically along the y-axis, starting from the origin towards the IR, while the locations of all the other nodes are fixed. As the relay moves, it becomes closer to the IR and farther from the source. We can see from Fig. 6 that

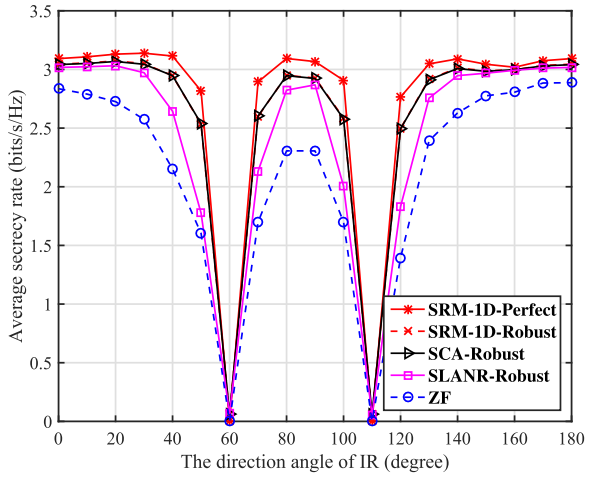

Fig. 7. Average secrecy rate versus the location of IR for $N = 6$, $M = 2$, $P_s = 30\text{dBm}$, $P_t = 30\text{dBm}$, $P_{\min} = 5\text{dBm}$, $\Delta\theta_{\max} = 6^\circ$.

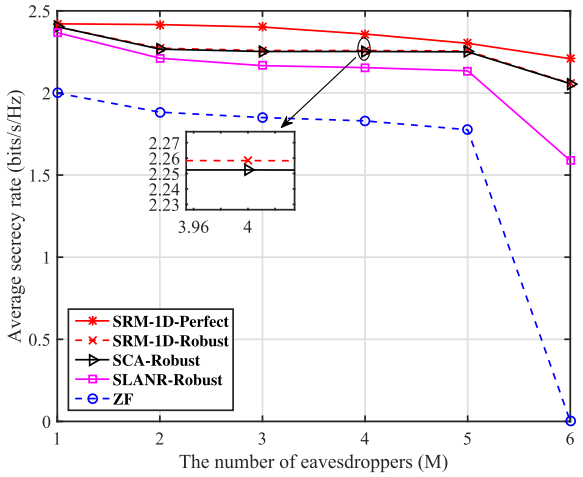

Fig. 8. Average secrecy rate versus the number of eavesdroppers for $N = 6$, $\{\theta_{re_1}, \theta_{re_2}, \theta_{re_3}, \theta_{re_4}, \theta_{re_5}, \theta_{re_6}\} = \{\frac{\pi}{3}, \frac{11\pi}{18}, \frac{3\pi}{4}, \frac{\pi}{6}, \frac{2\pi}{3}, \frac{4\pi}{9}\}$, $P_s = 30\text{dBm}$, $P_t = 30\text{dBm}$, $P_{\min} = 10\text{dBm}$, $\Delta\theta_{\max} = 6^\circ$.

for all the schemes, the secrecy rate increases first and then decreases. The secrecy rate increases because the received signal-to-noise ratio (SNR) increases as the relay moves to the IR. The secrecy rate decreases because, as the relay continues approaching the IR, it is getting farther away from the source node, which decreases the SNR of the IR. We can observe that the optimal point is $y_r = 30\text{m}$. Moreover, when $y_r = 60\text{m}$, it is observed that the secrecy rates of all schemes converge to the same points, because when the relay has a low SNR, all these schemes have a similar secrecy rate performance.

Fig. 7 shows the secrecy rate versus the direction angle of the IR. We assume that the IR moves on a circle and its direction angel varies from 0° to 180°. It can be seen that when the location of IR is the same as that of the eavesdroppers, the secrecy rate is zero for all schemes. This is because, in this case, IR and eavesdroppers receive the same confidential messages. In addition, for every directions that IR moves to, the secrecy rates of SRM-1D-Robust and SCA-Robust schemes are always close and superior to that of SLANR-Robust and ZF schemes.

Fig. 8 shows the secrecy rate versus the number of eavesdroppers. As seen from Fig. 8, when $M = 2$ and $M = 6$, the secrecy rate of the proposed algorithm decreases rapidly. This is because the second and sixth eavesdroppers are located near the DR. Moreover, when $M = 6$, the secrecy rate of the ZF scheme is 0. This is because, the degrees of freedom of the relay is 6 ($N = 6$), whereas the degrees of freedom at the eavesdroppers become 6 when $M = 6$. Therefore, there is no degrees of freedom left for the DR.

Fig. 9 studies the BER versus the direction angle. We employ quadrature phase shift keying (QPSK) modulation. As seen from Fig. 9, the BER performance in the desired direction of 90° is significantly better than in other directions for all cases. Observe from Fig. 9, that in the vicinity of the two eavesdroppers' directions, the BER performance is poor, since the signals in these two directions are contaminated by the AN. Thus the eavesdroppers cannot successfully receive the information destined to the IR.

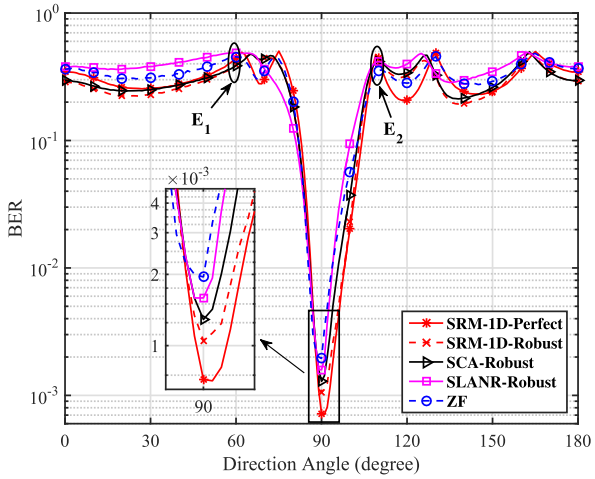

Fig. 9. The performance of BER versus direction angle for $N = 6$, $M = 2$, $P_s = 30\text{dBm}$, $P_t = 25\text{dBm}$, $P_{\min} = 5\text{dBm}$, $\Delta\theta_{\max} = 6^\circ$.

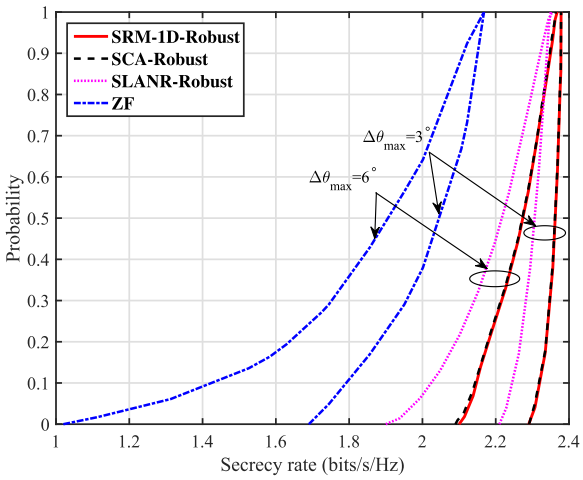

Fig. 10. CDF of the secrecy rate for $N = 6$, $M = 2$, $P_s = 30\text{dBm}$, $P_t = 25\text{dBm}$, $P_{\min} = 10\text{dBm}$.

Fig. 10 illustrates the cumulative density function (CDF) of the secrecy rate gleaned from 10000 samples of random angle errors, which follows the truncated Gaussian distribution.

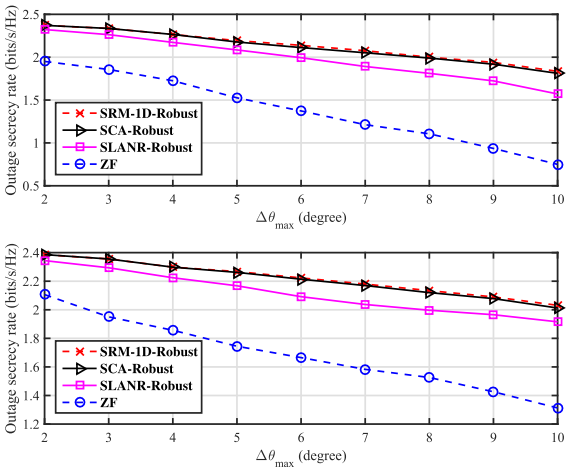

Fig. 11. Outage secrecy rate versus the maximum estimate error angle for $N = 6$, $M = 2$, $P_s = 30$dBm, $P_t = 30$dBm, $P_{\min} = 10$dBm, where the upper is 5% outage rate, and the lower is 20% outage rate.

It can be observed that the performance of the SCA-Robust and SRM-1D-Robust schemes is very close and significantly better than that of SLANR-Robust and ZF schemes. Specially, in the low probability range the ZF scheme has a significantly worse performance than the other three schemes. Additionally, we can see that the security associated with $\Delta\theta_{max} = 3^\circ$ is obviously better than that of $\Delta\theta_{max} = 6^\circ$ for all schemes.

Fig. 11 portrays the outage secrecy rate versus the maximum angle estimation error. We can see that the outage secrecy rates of 5% (the upper subplot of Fig. 11) and 20% (the lower subplot of Fig. 11) decrease slowly with the maximum angle estimation error for the proposed schemes, which shows the robustness of our proposed schemes. Moreover, the corresponding outage secrecy rate of 5% is less than that of 20%. For example, when $\Delta\theta_{max} = 10^\circ$, the outage secrecy rates corresponding to 5%-outage rate and 20%-outage rate of the SCA-Robust scheme are 1.8 bits/s/Hz and 2 bits/s/Hz, respectively.

V. Conclusions

In this paper, we investigated secure wireless information and power transfer based on DM in AF relay networks. Specifically, the robust information beamforming matrix and the AN covariance matrix were designed based on the SRM-1D scheme and on the Max-SLANR scheme. To solve the optimization problem of SRM, we proposed a twin-level optimization method that includes a 1D search and the SDR technique. Furthermore, we proposed a suboptimal solution for the SRM problem, which was based on the Max-SLANR criterion. Finally, we formulated a SRM problem, which was transformed into a SOCP problem, and solved by a low-complexity SCA method. Simulation results show that the performance of the SCA scheme is very close to that of the SRM-1D scheme in terms of its secrecy rate and BER, and compared to the ZF scheme, the SCA scheme and Max-SLANR schemes provide a significant performance improvement.

Appendix A
Derivation of $H_{re_m}(p,q)$

$H_{re_m}(p,q)$ can be expressed as

$$\begin{aligned}
&H_{re_m}(p,q)\\
&= \mathbb{E}_{\Delta\theta_{re_m}}\Big[\mathbf{h}_p(\hat{\theta}_{re_m}+\Delta\theta_{re_m})\\
&\quad\times \mathbf{h}_q^H(\hat{\theta}_{re_m}+\Delta\theta_{re_m})\Big]\\
&= \frac{g_{re_m}}{N}\int_{-\Delta\theta_{max}}^{\Delta\theta_{max}} e^{j\alpha_{pq}\cos(\hat{\theta}_{re_m}+\Delta\theta_{re_m})} f(\Delta\theta_{re_m})\, d(\Delta\theta_{re_m})\\
&= \frac{g_{re_m}}{N}\int_{-\Delta\theta_{max}}^{\Delta\theta_{max}} \exp\Big\{j\alpha_{pq}\big(\cos(\hat{\theta}_{re_m})\cos(\Delta\theta_{re_m})\\
&\quad-\sin(\hat{\theta}_{re_m})\sin(\Delta\theta_{re_m})\big)\Big\} f(\Delta\theta_{re_m})\, d(\Delta\theta_{re_m}),
\end{aligned} \tag{57}$$

where $\alpha_{pq} = \frac{2\pi(q-p)l}{\lambda}$. In general, we can use high-resolution and low-complexity ROOT-MUSIC methods to estimate the direction angle, and the estimation error is generally small [47]. Therefore, we get the following approximate expression using second-order Taylor expansion

$$\begin{aligned}
\sin(\Delta\theta_{re_m}) &\approx \Delta\theta_{re_m}\\
\cos(\Delta\theta_{re_m}) &\approx 1-\frac{\Delta\theta_{re_m}^2}{2}.
\end{aligned} \tag{58}$$

Substituting (58) into (57) yields

$$\begin{aligned}
H_{re_m}(p,q) &= \hat{H}_{re_m}(p,q)\int_{-\Delta\theta_{max}}^{\Delta\theta_{max}}\\
&\quad e^{-j\alpha_{pq}\left(\cos(\hat{\theta}_{re_m})\frac{\Delta\theta_{re_m}^2}{2}+\sin(\hat{\theta}_{re_m})\Delta\theta_{re_m}\right)}\\
&\quad\times f(\Delta\theta_{re_m})\, d(\Delta\theta_{re_m})\\
&= \hat{H}_{re_m}(p,q)\int_{-\Delta\theta_{max}}^{\Delta\theta_{max}} \left[\cos\left(\xi_{p,q}^m\right)-j\sin\left(\xi_{p,q}^m\right)\right]\\
&\quad f(\Delta\theta_{re_m})\, d(\Delta\theta_{re_m})\\
&= \Gamma_{1_m}(p,q)-j\Gamma_{2_m}(p,q),
\end{aligned} \tag{59}$$

where

$$\hat{H}_{re_m}(p,q) = \frac{g_{re_m}}{N}e^{j\alpha_{pq}\cos(\hat{\theta}_{re_m})} \tag{60}$$

represents the p-th row and q-th column entry of $\mathbf{h}(\hat{\theta}_{re_m})\mathbf{h}^H(\hat{\theta}_{re_m})$, and

$$\xi_{p,q}^m = \alpha_{pq}\left(\cos(\hat{\theta}_{re_m})\frac{\Delta\theta_{re_m}^2}{2}+\sin(\hat{\theta}_{re_m})\Delta\theta_{re_m}\right), \tag{61a}$$

$$\begin{aligned}
&\Gamma_{1_m}(p,q)\\
&\quad= \hat{H}_{re_m}(p,q)\int_{-\Delta\theta_{max}}^{\Delta\theta_{max}} \cos\left(\xi_{p,q}^m\right) f(\Delta\theta_{re_m})\, d(\Delta\theta_{re_m}),
\end{aligned} \tag{61b}$$

$$\begin{aligned}
&\Gamma_{2_m}(p,q)\\
&\quad= \hat{H}_{re_m}(p,q)\int_{-\Delta\theta_{max}}^{\Delta\theta_{max}} \sin\left(\xi_{p,q}^m\right) f(\Delta\theta_{re_m})\, d(\Delta\theta_{re_m}).
\end{aligned} \tag{61c}$$

Now the task is to derive the analytic expression of $\Gamma_{1_m}(p,q)$ and $\Gamma_{2_m}(p,q)$. To this end, we first expand the trigonometric

function into the following form

$$\begin{aligned}&\cos\left(\xi_{p,q}^{m}\right)\\&=\cos\left(\alpha_{pq}\cos(\hat{\theta}_{re_m})\frac{\Delta\theta_{re_m}^2}{2}+\alpha_{pq}\sin(\hat{\theta}_{re_m})\Delta\theta_{re_m}\right)\\&=\cos\left(\alpha_{pq}\cos(\hat{\theta}_{re_m})\frac{\Delta\theta_{re_m}^2}{2}\right)\cos\left(\alpha_{pq}\sin(\hat{\theta}_{re_m})\Delta\theta_{re_m}\right)\\&\quad-\sin\left(\alpha_{pq}\cos(\hat{\theta}_{re_m})\frac{\Delta\theta_{re_m}^2}{2}\right)\sin\left(\alpha_{pq}\sin(\hat{\theta}_{re_m})\Delta\theta_{re_m}\right).\end{aligned}\tag{62}$$

Then using the second-order Taylor series to approximate each term, we can rewrite (62) as

$$\begin{aligned}&\cos\left(\xi_{p,q}^{m}\right)\\&=\left(1-\frac{\alpha_{pq}^2\cos^2(\hat{\theta}_{re_m})\Delta\theta_{re_m}^4}{8}\right)\\&\quad\times\left(1-\frac{\alpha_{pq}^2\sin^2(\hat{\theta}_{re_m})\Delta\theta_{re_m}^2}{2}\right)\\&\quad-\left(\alpha_{pq}\cos(\hat{\theta}_{re_m})\frac{\Delta\theta_{re_m}^2}{2}\right)\left(\alpha_{pq}\sin(\hat{\theta}_{re_m})\Delta\theta_{re_m}\right)\\&\approx\left(1-\frac{1}{2}\alpha_{pq}^2\sin^2(\hat{\theta}_{re_m})\Delta\theta_{re_m}^2\right)\\&\quad-\left(\alpha_{pq}\cos(\hat{\theta}_{re_m})\frac{\Delta\theta_{re_m}^2}{2}\right)\left(\alpha_{pq}\sin(\hat{\theta}_{re_m})\Delta\theta_{re_m}\right).\end{aligned}\tag{63}$$

Since the last term in (63) is an odd function with respect to $\Delta\theta_{re_m}$, hence we have (64), shown at the top of the next page. Note that step (a) in (64) results from the following equation [48]

$$\int_0^x t^2e^{-q^2t^2}dt=\frac{1}{2q^3}\left(\frac{\sqrt{\pi}}{2}\mathrm{erf}(qx)-qxe^{-q^2x^2}\right),\tag{65}$$

where $\mathrm{erf}(x)$ represents the error function defined as

$$\mathrm{erf}(x)=\frac{2}{\sqrt{\pi}}\int_0^x e^{-t^2}dt.\tag{66}$$

Using a similar method as above, $\Gamma_{2_m}(p,q)$ can be approximated as (67), shown at the top of the next page. Combining (59), (64) and (67), we obtain the analytic expression of $H_{re_m}(p,q)$ and the proof is completed. ■

APPENDIX B
PROOF OF LEMMA 1

The optimization problem (28) can be rewritten as

$$\begin{aligned}\min_{\tilde{\mathbf{W}},\boldsymbol{\Omega}}\ &P_s\mathrm{Tr}(\mathbf{C}_1\tilde{\mathbf{W}})+\sigma^2\mathrm{Tr}(\tilde{\mathbf{W}})\\\text{s.t.}\ &-P_s\mathrm{Tr}(\mathbf{A}_1\tilde{\mathbf{W}})+\sigma^2\phi(\beta)\mathrm{Tr}(\mathbf{A}_2\tilde{\mathbf{W}})\\&+\phi(\beta)\mathbf{h}^H(\theta_{rd})\boldsymbol{\Omega}\mathbf{h}(\theta_{rd})+\phi(\beta)\sigma^2\le 0,\\&(25b),\ (25c),\ (25d),\quad\tilde{\mathbf{W}}\succeq\mathbf{0},\ \boldsymbol{\Omega}\succeq\mathbf{0}.\end{aligned}\tag{68}$$

Since the problem (68) satisfies Slater's constraint qualification [42], its objective function and constraints are convex, and the optimal solution must satisfy KKT conditions. The Lagrangian of (68) is given in (69), shown at the top of the next page, where $\mu,\nu_m,\eta,\zeta,\mathbf{S}_1$ and $\mathbf{S}_2$ denote the dual variables associated with the constraint in (68). Let $\tilde{\mathbf{W}}^\star,\boldsymbol{\Omega}^\star$ be the optimal primal variables and $\mu^\star,\nu_m^\star,\eta^\star,\zeta^\star,\mathbf{S}_1^\star,\mathbf{S}_2^\star$ be the dual variables. The KKT conditions related to the proof are given as follows

$$\begin{aligned}\mathbf{S}_1^\star=&\,P_s\mathbf{C}_1+\sigma^2\mathbf{I}_{N^2}-\mu^\star P_s\mathbf{A}_1+\mu^\star\sigma^2\phi(\beta)\mathbf{A}_2\\&+P_s\sum_{m=1}^{M}\nu_m^\star\mathbf{B}_{1_m}-\beta\sigma^2\sum_{m=1}^{M}\nu_m^\star\mathbf{B}_{2_m}+\eta^\star P_s\mathbf{C}_1\\&+\eta^\star\sigma^2\mathbf{I}_{N^2}-\zeta^\star P_s\mathbf{D}_1-\zeta^\star\sigma^2\mathbf{D}_2,\end{aligned}\tag{70a}$$

$$\begin{aligned}\mathbf{S}_2^\star=&\,\mu^\star\phi(\beta)\mathbf{h}(\theta_{rd})\mathbf{h}^H(\theta_{rd})-\beta\sum_{m=1}^{M}\nu_m^\star\mathbf{H}_{re_m}\\&+\eta^\star\mathbf{I}_N-\zeta^\star\mathbf{h}(\theta_{rp})\mathbf{h}^H(\theta_{rp}),\end{aligned}\tag{70b}$$

$$\mathbf{S}_1^\star\tilde{\mathbf{W}}^\star=\mathbf{0},\ \ \mathbf{S}_2^\star\boldsymbol{\Omega}^\star=\mathbf{0},\ \ \mathbf{S}_1^\star\succeq\mathbf{0},\ \ \mathbf{S}_2^\star\succeq\mathbf{0},\ \ \tilde{\mathbf{W}}\succeq\mathbf{0}.\tag{70c}$$

From (70b), we arrive at:

$$\begin{aligned}&\left(P_s\mathbf{h}^*(\theta_{sr})\mathbf{h}^T(\theta_{sr})+\sigma^2\mathbf{I}_N\right)\otimes\mathbf{S}_2^\star\\&=\mu^\star P_s\phi(\beta)\mathbf{A}_1\\&\quad+\mu^\star\sigma^2\phi(\beta)\mathbf{A}_2-\beta P_s\sum_{m=1}^{M}\nu_m^\star\mathbf{B}_{1_m}-\beta\sigma^2\sum_{m=1}^{M}\nu_m^\star\mathbf{B}_{2_m}\\&\quad+\eta^\star P_s\mathbf{C}_1+\eta^\star\sigma^2\mathbf{I}_{N^2}-\zeta^\star P_s\mathbf{D}_1-\zeta^\star\sigma^2\mathbf{D}_2.\end{aligned}\tag{71}$$

Substituting (71) into (70a), we have

$$\mathbf{S}_1^\star+\mu^\star P_s\left[\phi(\beta)+1\right]\mathbf{A}_1=\boldsymbol{\Xi},\tag{72}$$

where

$$\begin{aligned}\boldsymbol{\Xi}=&\,\sigma^2\mathbf{I}_{N^2}+P_s\mathbf{C}_1+P_s(\beta+1)\sum_{m=1}^{M}\nu_m^\star\mathbf{B}_{1_m}\\&+\left[P_s\mathbf{h}^*(\theta_{sr})\mathbf{h}^T(\theta_{sr})+\sigma^2\mathbf{I}_N\right]\otimes\mathbf{S}_2^\star.\end{aligned}\tag{73}$$

Let us multiply both sides of (72) by $\tilde{\mathbf{W}}^\star$ and substitute the first term of (70c) into the resultant equation, yielding:

$$\mu^\star P_s\left(\phi(\beta)+1\right)\mathbf{A}_1\tilde{\mathbf{W}}^\star=\boldsymbol{\Xi}\tilde{\mathbf{W}}^\star.\tag{74}$$

Since $\left(P_s\mathbf{h}^*(\theta_{sr})\mathbf{h}^T(\theta_{sr})+\sigma^2\mathbf{I}_N\right)$ is a Hermitian positive definite matrix, and $\mathbf{S}_2^\star\succeq\mathbf{0}$, according to the fact that [49]

$$\lambda(\mathbf{X}\otimes\mathbf{Y})=\{\mu_i\gamma_j,\mu_i\in\lambda(\mathbf{X}),\gamma_j\in\lambda(\mathbf{Y})\},\tag{75}$$

we have

$$\left[P_s\mathbf{h}^*(\theta_{sr})\mathbf{h}^T(\theta_{sr})+\sigma^2\mathbf{I}_N\right]\otimes\mathbf{S}_2^\star\succeq\mathbf{0},\tag{76}$$

where $\lambda(\bullet)$ denotes the set of matrix eigenvalues. Upon observing that the first term in (73) is the identity matrix and the other three terms are Hermitian semidefinite matrices, we have $\boldsymbol{\Xi}\succ\mathbf{0}$. By exploiting the fact that $\mathrm{rank}(\mathbf{AB})\le\min\{\mathrm{rank}(\mathbf{A}),\mathrm{rank}(\mathbf{B})\}$, we obtain

$$\mathrm{rank}(\boldsymbol{\Xi}\tilde{\mathbf{W}}^\star)=\mathrm{rank}(\tilde{\mathbf{W}}^\star)\le\mathrm{rank}(\mu^\star P_s\left(\phi(\beta)+1\right)\mathbf{A}_1).\tag{77}$$

Combining (74) with (77) and considering that $\mathbf{A}_1$ is a rank-one matrix, we conclude that $\mathrm{rank}(\tilde{\mathbf{W}}^\star)=1$ for $\mu^\star>0$, $\mathrm{rank}(\tilde{\mathbf{W}}^\star)=0$ for $\mu^\star=0$. However, $\tilde{\mathbf{W}}^\star=\mathbf{0}$ corresponds to no signal transmission. Hence we can conclude that $\mathrm{rank}(\tilde{\mathbf{W}}^\star)=1$, and the proof is completed. ■

$$\Gamma_{1_m}(p,q) \approx \hat{H}_{re_m}(p,q)\int_{-\Delta\theta_{max}}^{\Delta\theta_{max}}\left(1-\frac{1}{2}\alpha_{pq}^2\sin^2(\hat{\theta}_{re_m})\Delta\theta_{re_m}^2\right)f\left(\Delta\theta_{re_m}\right)d(\Delta\theta_{re_m})$$
$$\overset{(a)}{=} \frac{\hat{H}_{re_m}(p,q)}{K_{e_m}}\left(\mathrm{erf}(\frac{\Delta\theta_{max}}{\sqrt{2}\sigma_\theta})-\alpha_{pq}^2\sin^2(\hat{\theta}_{re_m})\sigma_\theta^2\left(\frac{1}{2}\mathrm{erf}(\frac{\Delta\theta_{max}}{\sqrt{2}\sigma_\theta})-\frac{\Delta\theta_{max}}{\sqrt{2\pi}\sigma_\theta}e^{-\frac{1}{2\sigma_\theta^2}\Delta\theta_{max}^2}\right)\right), \quad (64)$$

$$\Gamma_{2_m}(p,q) \approx \hat{H}_{re_m}(p,q)\int_{-\Delta\theta_{max}}^{\Delta\theta_{max}}\left(\frac{1}{2}\alpha_{pq}\cos(\hat{\theta}_{re_m})\Delta\theta_{re_m}^2\right)f\left(\Delta\theta_{re_m}\right)d(\Delta\theta_{re_m})$$
$$= \frac{\hat{H}_{re_m}(p,q)\alpha_{pq}\cos(\hat{\theta}_{re_m})\sigma_\theta^2}{K_{e_m}}\left(\frac{1}{2}\mathrm{erf}(\frac{\Delta\theta_{max}}{\sqrt{2}\sigma_\theta})-\frac{\Delta\theta_{max}}{\sqrt{2\pi}\sigma_\theta}e^{-\frac{1}{2\sigma_\theta^2}\Delta\theta_{max}^2}\right). \quad (67)$$

$$L(\tilde{\mathbf{W}},\mathbf{\Omega},\mu,\nu_m,\eta,\zeta,\mathbf{S}_1,\mathbf{S}_2)$$
$$= P_s\mathrm{Tr}(\mathbf{C}_1\tilde{\mathbf{W}})+\sigma^2\mathrm{Tr}(\tilde{\mathbf{W}})+\mu\left(-P_s\mathrm{Tr}(\mathbf{A}_1\tilde{\mathbf{W}})+\sigma^2\phi(\beta)\mathrm{Tr}(\mathbf{A}_2\tilde{\mathbf{W}})+\phi(\beta)\mathbf{h}^H(\theta_{rd})\mathbf{\Omega}\mathbf{h}(\theta_{rd})+\phi(\beta)\sigma^2\right)$$
$$+\sum_{m=1}^{M}\nu_m\left(P_s\mathrm{Tr}(\mathbf{B}_{1_m}\tilde{\mathbf{W}})-\beta\sigma^2\mathrm{Tr}(\mathbf{B}_{2_m}\tilde{\mathbf{W}})-\beta\mathrm{Tr}(\bar{\mathbf{H}}_{re_m}\mathbf{\Omega})-\beta\sigma^2\right)+\eta\left(P_s\mathrm{Tr}(\mathbf{C}_1\tilde{\mathbf{W}})+\sigma^2\mathrm{Tr}(\tilde{\mathbf{W}})+\mathrm{Tr}(\mathbf{\Omega})-P_t\right)$$
$$-\zeta\left(P_s\mathrm{Tr}(\mathbf{D}_1\tilde{\mathbf{W}})+\sigma^2\mathrm{Tr}(\mathbf{D}_2\tilde{\mathbf{W}})+\mathbf{h}^H(\theta_{rp})\mathbf{\Omega}\mathbf{h}(\theta_{rp})-\frac{P_{min}}{\rho}\right)-\mathrm{Tr}(\mathbf{S}_1\tilde{\mathbf{W}})-\mathrm{Tr}(\mathbf{S}_2\mathbf{\Omega}). \quad (69)$$

APPENDIX C
PROOF OF LEMMA 2

Since the problem (36) satisfies Slater's constraint qualification [42], its objective function and constraints are convex, and the optimal solution must satisfy KKT conditions. The Lagrangian associated with the problem (36) is given by

$$L(\tilde{\mathbf{W}},\mathbf{\Omega},\mu,\eta,\zeta,\mathbf{S}_1,\mathbf{S}_2)$$
$$= P_s\mathrm{Tr}(\mathbf{C}_1\tilde{\mathbf{W}})+\sigma^2\mathrm{Tr}(\tilde{\mathbf{W}})$$
$$+\mu\Big(-P_s\mathrm{Tr}(\mathbf{A}_1\tilde{\mathbf{W}})+\phi\sum_{m=1}^{M}P_s\mathrm{Tr}(\mathbf{B}_{1_m}\tilde{\mathbf{W}})$$
$$+\phi\mathbf{h}^H(\theta_{rd})\mathbf{\Omega}\mathbf{h}(\theta_{rd})+\phi\sigma^2\mathrm{Tr}(\mathbf{A}_2\tilde{\mathbf{W}})+\phi\sigma^2\Big)$$
$$+\eta\left(P_s\mathrm{Tr}(\mathbf{C}_1\tilde{\mathbf{W}})+\sigma^2\mathrm{Tr}(\tilde{\mathbf{W}})+\mathrm{Tr}(\mathbf{\Omega})-P_t\right)$$
$$-\zeta\Big(P_s\mathrm{Tr}(\mathbf{D}_1\tilde{\mathbf{W}})+\sigma^2\mathrm{Tr}(\mathbf{D}_2\tilde{\mathbf{W}})+\mathbf{h}^H(\theta_{rp})\mathbf{\Omega}\mathbf{h}(\theta_{rp})$$
$$-\frac{P_{min}}{\rho}\Big)-\mathrm{Tr}(\mathbf{S}_1\tilde{\mathbf{W}})-\mathrm{Tr}(\mathbf{S}_1\tilde{\mathbf{W}})-\mathrm{Tr}(\mathbf{S}_2\mathbf{\Omega}), \quad (78)$$

where $\mu,\eta,\zeta,\mathbf{S}_1$ and $\mathbf{S}_2$ are dual variables associated with the constraint in (36), while $\tilde{\mathbf{W}}^\star,\mathbf{\Omega}^\star$ are the optimal primal variables and $\mu^\star,\eta^\star,\zeta^\star,\mathbf{S}_1^\star,\mathbf{S}_2^\star$ are dual variables. The KKT conditions that are relevant to the proof are given by

$$\mathbf{S}_1^\star = P_s\mathbf{C}_1-\mu^\star P_s\mathbf{A}_1+\mu^\star\phi\sigma^2\mathbf{A}_2+\mu^\star\phi P_s\sum_{m=1}^{M}\mathbf{B}_{1_m}$$
$$+\sigma^2\mathbf{I}_{N^2}+\eta^\star P_s\mathbf{C}_1+\eta^\star\sigma^2\mathbf{I}_{N^2}-\zeta^\star P_s\mathbf{D}_1-\zeta^\star\sigma^2\mathbf{D}_2, \quad (79a)$$

$$\mathbf{S}_2^\star = \mu^\star\phi\mathbf{h}(\theta_{rd})\mathbf{h}^H(\theta_{rd})+\eta^\star\mathbf{I}_N-\zeta^\star\mathbf{h}(\theta_{rp})\mathbf{h}^H(\theta_{rp}), \quad (79b)$$

$$\mathbf{S}_1^\star\tilde{\mathbf{W}}^\star=\mathbf{0},\quad \mathbf{S}_2^\star\mathbf{\Omega}^\star=\mathbf{0},\ \mathbf{S}_1^\star\succeq\mathbf{0},\ \mathbf{S}_2^\star\succeq\mathbf{0},\ \tilde{\mathbf{W}}\succeq\mathbf{0}. \quad (79c)$$

From (79b), we get

$$\left[P_s\mathbf{h}^*(\theta_{sr})\mathbf{h}^T(\theta_{sr})+\sigma^2\mathbf{I}_N\right]\otimes\mathbf{S}_2^\star$$
$$=\mu^\star P_s\phi\mathbf{A}_1+\mu^\star\sigma^2\phi\mathbf{A}_2+\eta^\star P_s\mathbf{C}_1$$
$$+\eta^\star\sigma^2\mathbf{I}_{N^2}-\zeta^\star P_s\mathbf{D}_1-\zeta^\star\sigma^2\mathbf{D}_2. \quad (80)$$

Substituting (80) into (79a), we have

$$\mathbf{S}_1^\star+\mu^\star P_s\left(1+\phi\right)\mathbf{A}_1=\mathbf{\Xi}, \quad (81)$$

where

$$\mathbf{\Xi}=\sigma^2\mathbf{I}_{N^2}+P_s\mathbf{C}_1+\mu^\star\phi P_s\sum_{m=1}^{M}\mathbf{B}_{1_m}$$
$$+\left[P_s\mathbf{h}^*(\theta_{sr})\mathbf{h}^T(\theta_{sr})+\sigma^2\mathbf{I}_N\right]\otimes\mathbf{S}_2^\star. \quad (82)$$

It is clear from (82) that $\mathbf{\Xi}$ is a Hermitian positive definite matrix. The remaining steps of the proof are similar to the *Lemma 1* and is omitted here. The proof is completed. ■

REFERENCES

[1] Q. Wu, W. Chen, D. W. K. Ng, and R. Schober, "Spectral and energy-efficient wireless powered IoT networks: NOMA or TDMA?" *IEEE Trans. Veh. Technol.*, vol. 67, no. 7, pp. 6663–6667, Jul. 2018.

[2] H. Son and B. Clerckx, "Joint beamforming design for multi-user wireless information and power transfer," *IEEE Trans. Wireless Commun.*, vol. 13, no. 11, pp. 6397–6409, Nov. 2014.

[3] Z. Chu, Z. Zhu, M. Johnston, and S. Y. Le Goff, "Simultaneous wireless information power transfer for MISO secrecy channel," *IEEE Trans. Veh. Technol.*, vol. 65, no. 9, pp. 6913–6925, Sep. 2016.

[4] H. Zhang, Y. Huang, C. Li, and L. Yang, "Secure beamforming design for SWIPT in MISO broadcast channel with confidential messages and external eavesdroppers," *IEEE Trans. Wireless Commun.*, vol. 15, no. 11, pp. 7807–7819, Nov. 2016.

[5] D. W. K. Ng, E. S. Lo, and R. Schober, "Robust beamforming for secure communication in systems with wireless information and power transfer," *IEEE Trans. Wireless Commun.*, vol. 13, no. 8, pp. 4599–4615, Aug. 2013.

[6] W. Wu and B. Wang, "Robust secrecy beamforming for wireless information and power transfer in multiuser MISO communication system," *EURASIP J. Wireless Commun. Netw.*, vol. 2015, no. 1, pp. 161–171, Jun. 2015.

[7] M. R. A. Khandaker and K.-K. Wong, "Robust secrecy beamforming with energy-harvesting eavesdroppers," *IEEE Wireless Commun. Lett.*, vol. 4, no. 1, pp. 10–13, Feb. 2015.
[8] W. Mei, Z. Chen, and J. Fang, "Artificial noise aided energy efficiency optimization in MIMOME system with SWIPT," *IEEE Commun. Lett.*, vol. 21, no. 8, pp. 1795–1798, Aug. 2017.
[9] X. Zhou, R. Zhang, and C. K. Ho, "Wireless information and power transfer: Architecture design and rate-energy tradeoff," *IEEE Trans. Commun.*, vol. 61, no. 11, pp. 4754–4767, Nov. 2013.
[10] R. Zhang and C. K. Ho, "MIMO broadcasting for simultaneous wireless information and power transfer," *IEEE Trans. Wireless Commun.*, vol. 12, no. 5, pp. 1989–2001, May 2013.
[11] Q. Wu, G. Y. Li, W. Chen, D. W. K. Ng, and R. Schober, "An overview of sustainable green 5G networks," *IEEE Wireless Commun.*, vol. 24, no. 4, pp. 72–80, Aug. 2017.
[12] Q. Wu, M. Tao, D. W. K. Ng, W. Chen, and R. Schober, "Energy-efficient resource allocation for wireless powered communication networks," *IEEE Trans. Wireless Commun.*, vol. 15, no. 3, pp. 2312–2327, Mar. 2016.
[13] K. Xiong, P. Fan, C. Zhang, and K. B. Letaief, "Wireless information and energy transfer for two-hop non-regenerative MIMO-OFDM relay networks," *IEEE J. Sel. Areas Commun.*, vol. 33, no. 8, pp. 1595–1611, Aug. 2015.
[14] B. Li and Y. Rong, "AF MIMO relay systems with wireless powered relay node and direct link," *IEEE Trans. Commun.*, vol. 66, no. 4, pp. 1508–1519, Apr. 2018.
[15] X. Chen, D. W. K. Ng, and H.-H. Chen, "Secrecy wireless information and power transfer: Challenges and opportunities," *IEEE Wireless Commun.*, vol. 23, no. 2, pp. 54–61, Apr. 2015.
[16] Y. Zou, J. Zhu, X. Wang, and L. Hanzo, "A survey on wireless security: Technical challenges, recent advances, and future trends," *Proc. IEEE*, vol. 104, no. 9, pp. 1727–1765, Sep. 2015.
[17] Y. Zou, B. Champagne, W. P. Zhu, and L. Hanzo, "Relay-selection improves the security-reliability trade-off in cognitive radio systems," *IEEE Trans. Commun.*, vol. 63, no. 1, pp. 215–228, Jan. 2014.
[18] Y. Huang and B. Clerckx, "Relaying strategies for wireless-powered MIMO relay networks," *IEEE Trans. Wireless Commun.*, vol. 15, no. 9, pp. 6033–6047, Sep. 2016.
[19] P. Liu, S. Gazor, I. M. Kim, and D. I. Kim, "Noncoherent relaying in energy harvesting communication systems," *IEEE Trans. Wireless Commun.*, vol. 14, no. 12, pp. 6940–6954, Dec. 2015.
[20] Q. Li, Q. Zhang, and J. Qin, "Secure relay beamforming for simultaneous wireless information and power transfer in nonregenerative relay networks," *IEEE Trans. Veh. Technol.*, vol. 63, no. 5, pp. 2462–2467, Jun. 2014.
[21] A. Salem, K. A. Hamdi, and K. M. Rabie, "Physical layer security with RF energy harvesting in af multi-antenna relaying networks," *IEEE Trans. Commun.*, vol. 64, no. 7, pp. 3025–3038, Jul. 2016.
[22] Q. Li, Q. Zhang, and J. Qin, "Secure relay beamforming for SWIPT in amplify-and-forward two-way relay networks," *IEEE Trans. Veh. Technol.*, vol. 65, no. 11, pp. 9006–9019, Nov. 2016.
[23] B. Li, Y. Rong, J. Sun, and K. L. Teo, "A distributionally robust linear receiver design for multi-access space-time block coded MIMO systems," *IEEE Trans. Wireless Commun.*, vol. 16, no. 1, pp. 464–474, Jan. 2017.
[24] B. Li, Y. Rong, J. Sun, and K. L. Teo, "A distributionally robust minimum variance beamformer design," *IEEE Signal Process. Lett.*, vol. 25, no. 1, pp. 105–109, Jan. 2018.
[25] H. Xing, K.-K. Wong, Z. Chu, and A. Nallanathan "To harvest and jam: A paradigm of self-sustaining friendly jammers for secure AF relaying," *IEEE Trans. Signal Process.*, vol. 63, no. 24, pp. 6616–6631, Dec. 2015.
[26] Y. Feng, Z. Yang, W.-P. Zhu, Q. Li, and B. Lv, "Robust cooperative secure beamforming for simultaneous wireless information and power transfer in amplify-and-forward relay networks," *IEEE Trans. Veh. Technol.*, vol. 66, no. 3, pp. 2354–2366, Mar. 2017.
[27] B. Li, Z. Fei, Z. Chu, and Y. Zhang, "Secure transmission for heterogeneous cellular networks with wireless information and power transfer," *IEEE Syst. J.*, to be published. [Online]. Available: https://ieeexplore.ieee.org/document/7956165, doi: 10.1109/JSYST.2017.2713881.
[28] H. Niu, B. Zhang, D. Guo, and Y. Huang, "Joint robust design for secure AF relay networks with SWIPT," *IEEE Access*, vol. 5, pp. 9369–9377, Apr. 2017.
[29] B. Li, Z. Fei, and H. Chen, "Robust artificial noise-aided secure beamforming in wireless-powered non-regenerative relay networks," *IEEE Access*, vol. 4, pp. 7921–7929, 2016.
[30] M. P. Daly and J. T. Bernhard, "Directional modulation technique for phased arrays," *IEEE Trans. Antennas Propag.*, vol. 57, no. 9, pp. 2633–2640, Sep. 2009.
[31] Y. Ding and V. F. Fusco, "A vector approach for the analysis and synthesis of directional modulation transmitters," *IEEE Trans. Antennas Propag.*, vol. 62, no. 1, pp. 361–370, Jan. 2014.
[32] Y. Ding and V. Fusco, "Orthogonal vector approach for synthesis of multi-beam directional modulation transmitters," *IEEE Antennas Wireless Propag. Lett.*, vol. 14, pp. 1330–1333, Feb. 2015.
[33] J. S. Hu, F. Shu, and J. Li, "Robust synthesis method for secure directional modulation with imperfect direction angle," *IEEE Commun. Lett.*, vol. 20, no. 6, pp. 1084–1087, Jun. 2016.
[34] F. Shu, X. Wu, J. Li, R. Chen, and B. Vucetic, "Robust synthesis scheme for secure multi-beam directional modulation in broadcasting systems," *IEEE Access*, vol. 4, pp. 6614–6623, Oct. 2016.
[35] Q. Li, Y. Yang, W. K. Ma, M. Lin, J. Ge, and J. Lin, "Robust cooperative beamforming and artificial noise design for physical-layer secrecy in AF multi-antenna multi-relay networks," *IEEE Trans. Signal Process.*, vol. 63, no. 1, pp. 206–220, Jan. 2015.
[36] L. Liu, R. Zhang, and K.-C. Chua, "Secrecy wireless information and power transfer with MISO beamforming," *IEEE Trans. Signal Process.*, vol. 62, no. 7, pp. 1850–1863, Apr. 2014.
[37] L. Dong, Z. Han, A. P. Petropulu, and H. V. Poor, "Improving wireless physical layer security via cooperating relays," *IEEE Trans. Signal Process.*, vol. 58, no. 3, pp. 1875–1888, Mar. 2010.
[38] C. Liu, G. Geraci, N. Yang, J. Yuan, and R. Malaney, "Beamforming for MIMO Gaussian wiretap channels with imperfect channel state information," in *Proc. IEEE Global Commun. Conf.*, Dec. 2013, pp. 3253–3258.
[39] A. Mukherjee and A. L. Swindlehurst, "Robust beamforming for security in MIMO wiretap channels with imperfect CSI," *IEEE Trans. Signal Process.*, vol. 59, no. 1, pp. 351–361, Jan. 2011.
[40] A. M. Alam, P. Mary, J.-Y. Baudais, and X. Lagrange, "Asymptotic analysis of area spectral efficiency and energy efficiency in PPP networks with SLNR precoder," *IEEE Trans. Commun.*, vol. 65, no. 7, pp. 3172–3185, Jul. 2017.
[41] A. Charnes and W. W. Cooper, "Programming with linear fractional functionals," *Naval Res. Logistics Quart.*, vol. 9, nos. 3–4, pp. 181–186, 1962.
[42] S. Boyd and L. Vandenberghe, *Convex Optimization*. Cambridge U.K.: Cambridge Univ. Press, 2004.
[43] F. Shu, J. Tong, X. You, G. U. Chen, and W. U. Jiajun, "Adaptive robust Max-SLNR precoder for MU-MIMO-OFDM systems with imperfect CSI," *Sci. China Inf. Sci.*, vol. 59, no. 6, pp. 1–14, Jul. 2016.
[44] A. A. Nasir, H. D. Tuan, T. Q. Duong, and H. V. Poor, "Secrecy rate beamforming for multicell networks with information and energy harvesting," *IEEE Trans. Signal Process.*, vol. 65, no. 3, pp. 677–689, Feb. 2017.
[45] A. Zappone, E. Björnson, L. Sanguinetti, and E. Jorswieck, "Globally optimal energy-efficient power control and receiver design in wireless networks," *IEEE Trans. Signal Process.*, vol. 65, no. 11, pp. 2844–2859, Jun. 2017.
[46] K.-Y. Wang, A. Man-Cho So, T.-H. Chang, W.-K. Ma, and C.-Y. Chi, "Outage constrained robust transmit optimization for multi-user MISO downlinks: Tractable approximations by conic optimization," *IEEE Trans. Signal Process.*, vol. 62, no. 21, pp. 5690–5705, Nov. 2014.
[47] F. Shu *et al.*, "Low-complexity and high-resolution DOA estimation for hybrid analog and digital massive MIMO receive array," *IEEE Trans. Commun.*, vol. 66, no. 6, pp. 2487–2501, Jun. 2018.
[48] I. S. Gradshteyn and I. M. Ryzhik, *Table of Integrals, Series, and Products*, 7th ed. San Diego, CA, USA: Academic, 2007.
[49] G. H. Golub and C. F. Van Loan, *Matrix computations*. Baltimore, MD, USA: The Johns Hopkins Univ. Press, 1996.

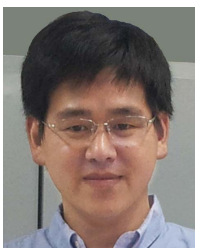

Xiaobo Zhou received the M.S. degree from the School of Electronic Science and Engineering, Anhui University, China, in 2010. He is currently pursuing the Ph.D. degree with the School of Electronic and Optical Engineering, Nanjing University of Science and Technology. Since 2010, he has been a faculty member with the School of Physics and Electronic Engineering, Fuyang Normal University. His main research interests are physical layer security, energy harvesting, and unmanned aerial vehicle communications.

Jun Li (M'09–SM'16) received the Ph.D. degree in electronic engineering from Shanghai Jiao Tong University, Shanghai, China, in 2009. In 2009, he was with the Department of Research and Innovation, Alcatel Lucent Shanghai Bell, as a Research Scientist. Since 2015, he has been with the School of Electronic and Optical Engineering, Nanjing University of Science and Technology, Nanjing, China. His research interests include network information theory, channel coding theory, wireless network coding, and cooperative communications.

Feng Shu (M'16) was born in 1973. He received the Ph.D. degree from the Fuyang Teaching College, Fuyang, China, in 1994, the M.S. degree from the Xidian University, Xi'an, China, in 1997, and the B.S. degree from the Southeast University, Nanjing, in 2002. From 2003 to 2005, he was a Post-Doctoral Researcher with the National Key Mobile Communication Lab, Southeast University. From 2009 to 2010, he held a visiting post-doctoral position at the University of Texas at Dallas. In 2005, he joined the School of Electronic and Optical Engineering, Nanjing University of Science and Technology, Nanjing, China, where he is currently a Professor, and also a supervisor of Ph.D. and graduate students. He is also with the Fujian Agriculture and Forestry University, and was awarded with Mingjian Scholar Chair Professor in Fujian. His research interests include wireless networks, wireless location, and array signal processing. He has published about 200 scientific and conference papers, of which over 100 are in archival journals, including over 50 papers on IEEE Journals and 70 SCI-indexed papers. He holds four Chinese patents. He is currently serving as an Editor for the IEEE ACCESS. He has served as the Session Chair or the Technical Program Committee Member for various international conferences such as IEEE WCSP 2016 and IEEE VTC 2016.

Qingqing Wu (S'13–M'16) received the B.Eng. degree from the South China University of Technology in 2012, and the Ph.D. degree in electronic engineering from the Shanghai Jiao Tong University (SJTU), China, in 2016. He is currently a Research Fellow with the National University of Singapore. His research interests include intelligent reflecting surface, energy-efficient wireless communications, wireless power transfer, and unmanned aerial vehicle communications. He has served as a TPC member for the IEEE ICC, Globecom, WCNC, VTC, APCC, and WCSP. He was a recipient of the Outstanding Ph.D. Thesis Funding at SJTU in 2016 and the Best Ph.D. Thesis Award of the China Institute of Communications in 2017. He received the IEEE WCSP Best Paper Award in 2015, the Exemplary Reviewer of IEEE Communications Letters in 2016 and 2017, respectively, and the Exemplary Reviewer of the IEEE TRANSACTIONS ON COMMUNICATIONS and the IEEE TRANSACTIONS ON WIRELESS COMMUNICATIONS in 2017.

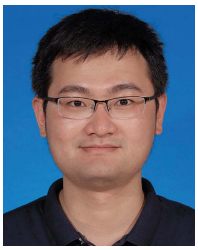

Yongpeng Wu (S'08–M'13–SM'17) received the B.S. degree in telecommunication engineering from Wuhan University, Wuhan, China, in 2007, and the Ph.D. degree in communication and signal processing with the National Mobile Communications Research Laboratory, Southeast University, Nanjing, China, in 2013. He was a Senior Research Fellow with the Institute for Communications Engineering, Technical University of Munich, Germany, and also the Humboldt Research Fellow and the Senior Research Fellow with the Institute for Digital Communications, University Erlangen-Nürnberg, Germany. He is currently a Tenure-Track Associate Professor with the Department of Electronic Engineering, Shanghai Jiao Tong University, China. During his Ph.D. studies, he conducted co-operative research at the Department of Electrical Engineering, Missouri University of Science and Technology, Rolla, MO, USA. His research interests include massive MIMO/MIMO systems, physical layer security, signal processing for wireless communications, and multivariate statistical theory.

Wen Chen received the B.S. and M.S. degrees from Wuhan University, China, in 1990 and 1993, respectively, and the Ph.D. degree from the University of Electro-Communications, Tokyo, Japan, in 1999. He was a Research Fellow of the Japan Society for the Promotion of Sciences from 1999 to 2001. In 2001, he joined the University of Alberta, Canada, as a Post-Doctoral Fellow, and then a Research Associate. Since 2006, he has been a Full Professor with the Department of Electronic Engineering, Shanghai Jiao Tong University, China, where he is also the Director of the Institute for Signal Processing and Systems. From 2014 to 2015, he was the Dean of the School of Electronics Engineering and Automations, Guilin University of Electronic Technology. Since 2016, he has been the Chairman of the SJTU Intellectual Property Management Corporation. He is a board member of the Shanghai Institute of Electronics in 2008, and the Chair of the IEEE VTS Shanghai Chapter. His research interests include multiple access, coded cooperation, and green heterogeneous networks. He is the Chair of the IEEE Vehicular Technology Society Shanghai Chapter. He is an Editor of the IEEE TRANSACTIONS ON WIRELESS COMMUNICATIONS, the IEEE TRANSACTIONS ON COMMUNICATIONS, and the IEEE ACCESS.

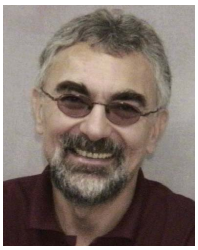

Lajos Hanzo (M'91–SM'92–F'04) received the D.Sc. and Ph.D. degrees in electronics from the Technical University of Budapest in 1976 and 1983, respectively. In 2009, he received the Honorary Doctorate from the Technical University of Budapest, and the University of Edinburgh in 2015. In 2016, he was admitted to the Hungarian Academy of Science. During his 40-year career in tele-communications, he has held various research and academic posts in Hungary, Germany, and the U.K. Since 1986, he has been with the School of Electronics and Computer Science, University of Southampton, U.K., where he holds the position of Chair in telecommunications. He has successfully supervised 112 Ph.D. students, co-authored 18 John Wiley/IEEE Press books on mobile radio communications totaling in excess of 10 000 pages, published 1771 research contributions at IEEE Xplore, and presented keynote lectures. He has received a number of distinctions. He has acted both as the TPC and General Chair of the IEEE conferences. He is currently directing a 60-strong academic research team, working on a range of research projects in the field of wireless multimedia communications sponsored by industry, the Engineering and Physical Sciences Research Council (EPSRC) UK, the European Research Council's Advanced Fellow Grant, and the Royal Society's Wolfson Research Merit Award. He is an enthusiastic supporter of the industrial and academic liaison, and he offers a range of industrial courses. He is also the Governor of the IEEE ComSoc and VTS. From 2008 to 2012, he was the Editor-in-Chief of the IEEE Press and also a Chaired Professor at Tsinghua University, Beijing.